LEPTONIC DIPOLE TRANSITIONS: A NEW SIGNATURE FOR PHYSICS BEYOND THE STANDARD MODEL

LEPTONIC DIPOLE TRANSITIONS: A NEW SIGNATURE FOR PHYSICS BEYOND THE STANDARD MODEL

By

ROBIN J TUNLEY, B.Sc.

A Thesis
Submitted to the School of Graduate Studies
in Partial Fulfillment of the Requirements
for the Degree
Master of Science

McMaster University

MASTER OF SCIENCE (2012) McMaster University
(Physics) Hamilton, Ontario

TITLE: Leptonic Dipole Transitions: A New Signature for Physics Beyond the Standard Model

AUTHOR: Robin J Tunley, B.Sc.(University of Guelph)

SUPERVISOR: Dr. I. Yavin

NUMBER OF PAGES: viii, 74

Abstract

In this work, we consider the addition of a single neutral massive vector boson to the Standard Model (SM). This boson, which we refer to as N^0, induces dipolar transitions between electrons and muons. We obtain bounds on the strength of its coupling and its mass: from the scattering process $e^+e^- \to \mu^+\mu^-$; from its contribution to muonium-antimuonium oscillations; and from its possible contribution to the rare muon decay $\mu^- \to e^-e^-e^+$. In particular, we examine the two cases where the mediator is both heavy and light compared with the scattering energies for $e^+e^- \to \mu^+\mu^-$, and place constraints on the relevant parameters based on their contributions to the cross section and the forward-backward asymmetry. For muonium-antimuonium oscillations, we consider only the case where the mediator is heavy compared to all other scales, reducing its effect to an effective contact interaction. Finally, we consider an $SU_L(2)$ invariant theory from which the N^0 interaction emerges, and find that flavour diagonal interactions also emerge, giving a tree-level path for the decay $\mu^- \to e^-e^-e^+$. We find that the heavy N^0 is not strongly constrained by this contribution, while the light N^0 is very strongly constrained by it. Very generally, we find that the heavy N^0 is much less constrained than other lepton flavour violating processes, while the constraints on the light N^0 vary in strength between processes.

Acknowledgements

First and foremost, I would like to thank my supervisor, Dr. Itay Yavin, for allowing me the opportunity to explore a subject which has captured my imagination since I was a teenager. For suggesting this topic, for guidance throughout the project, and for being a constant source of insight and inspiration, I am deeply grateful.

It has been a joy to work with the McMaster Particle Physics Group, most notably: Cliff Burgess, Allan Bayntun, Leo Van Nierop, Matthew Williams, Matt McCreadie and Joey Sham. It would have been a much rougher road without your support.

To my parents and family: I know it has been a long time since you've been able to help me with my homework, but your constant support and encouragement has not gone unnoticed. I could not have done this without you.

Thanks also to Itay Yavin and the McMaster Department of Physics and Astronomy for their financial support, and to the department staff who made my life easier at innumerable points throughout this masters, especially Alan Chen, Tina Stewart, Cheryl Johnston, Mara Esposto, and Rosemary McNeice.

"Beauty is worth its weight in sweat and toil."

Contents

1 Introduction and Motivation **1**

1.1 Lepton Flavour Violation 2

1.2 Bosons Mediating Lepton Flavour Violation 4

1.3 the Dipole Operator 6

1.A Appendix: Proof of the Gordon Identity 8

1.B Appendix: Proof of Electron Number Conservation in QED 9

2 Constraints from $e^+e^- \to \mu^+\mu^-$ **13**

2.1 The Cross Section 13

2.2 Heavy Mediator 19

2.3 Light Mediator 20

2.4 The Forward-Backward Asymmetry 21

2.5 Fits and Results 23

2.6 Comparison with Four-Fermion Constraints 26

2.A Appendix: Feynman Rules and Trace Technology 30

2.B Appendix: Mandelstam Variables and Kinematics 34

2.C Appendix: A_{FB} for the N^0 36

3 Constraints from Muonium - Antimuonium Oscillations **39**

3.1 N^0: The Heavy Case 41

3.2 The Feinberg-Weinberg Model 45

3.3 The Bilepton Model 47

3.A Appendix: Non-Relativistic Calculations 49

3.B Appendix: The Probability of Muonium Decaying as Antimuonium 52

4 Model Building **55**

4.1 Emergence of the Flavour-Mixing Signature 55

4.2 Generalized Leptonic Dipole Interaction 59

4.2.1 A Heavy N^0 59

4.2.2 A Light N^0 61

5 Conclusion and Discussion **63**

5.1 Summary of Results 63

5.2 Future Prospects 64

5.3 Conclusions 65

A Appendix: A (Very) Brief Introduction to the Standard Model **67**

List of Figures

1.1 the Feynman vertex associated with the addition of Equation 1.1 to the Standard Model Lagrangian. 2

1.2 Radiative corrections to the neutrino propagator giving rise to a neutrino magnetic dipole moment. Here, ϕ^+ is the unphysical Higgs scalar [7]. 7

2.1 Tree level processes for $e^+e^- \to \mu^+\mu^-$ in the Standard Model. The γ indicates an intermediate photon, while the Z indicates an intermediate Z boson. 13

2.2 The contribution from the N^0 boson to the process $e^+e^- \to \mu^+\mu^-$ 14

2.3 A reproduction of Figure 2 from [16]. Cross Sections for $e^+e^- \to \mu^+\mu^-$, in picobarnes above, and as a fraction of the SM prediction below, are shown in blue plotted against the center-of-mass energy $\sqrt{s}$. The black line is the theoretical prediction from Zfitter. 18

2.4 This is the only tree level diagram which contributes to $e^+e^- \to \mu^+\mu^-$ from the 4-fermion operators looked at by LEP [16]. 27

2.5 Kinematic conventions for a general two-body to two-body Feynman diagram. Here the dark circle is indicative of arbitrary processes occurring between the initial and final states. 35

2.6 Kinematic conventions in the center of mass frame, with the particle types specific to $e^+e^- \to \mu^+\mu^-$ scattering indicated. As mentioned in Section 2.1, θ is defined as the angle between the trajectories of p_1 and p_3. 35

3.1 The s-channel diagram contributing to muonium-antimuonium oscillation via the N^0. 41

3.2 The t-channel diagram contributing to muonium-antimuonium oscillation via the N^0. 42

3.3 The tree level process from the double charged X^{--} bilepton contributing to muonium-antimuonium oscillation [11]. 47

4.1 The decay of the muon into two electrons and a positron, facilitated by the generation preserving interaction of the generalized N^0 60

4.2 The decay of the muon into and electron and an on-shell N^0, facilitated by the flavour diagonal interactions present in equation 4.19. This decay route is possible only if the mass of the N^0 is lighter than that of the muon. 62

Chapter 1

Introduction and Motivation

The goal of this thesis is to consider the contribution of a neutral lepton flavour violating (LFV) interaction to the Standard Model (SM). This interaction is mediated by a massive spin-one gauge boson, similar to the Z boson in the electroweak theory of the SM, but which couples to leptons via a dipole transition given by the term

$$\mathcal{L}_{eff} = \frac{g\eta}{2\Lambda}\bar{e}\sigma^{\alpha\beta}\mu N_{\alpha\beta} + H.C., \tag{1.1}$$

where e is the electron field and μ is the muon field, η can take on values ± 1, and $N_{\mu\nu} = \partial_\mu N_\nu - \partial_\nu N_\mu$ is the gauge invariant field strength tensor for the massive vector field N_μ. The matrix $\sigma^{\mu\nu}$ is given in terms of the Dirac matrices γ^μ by

$$\sigma^{\mu\nu} = -\frac{i}{2}[\gamma^\mu, \gamma^\nu] = -\frac{i}{2}(\gamma^\mu\gamma^\nu - \gamma^\nu\gamma^\mu). \tag{1.2}$$

The parameter g gives a scale for the coupling and we adopt the convention of [8] by setting $g^2 = 4\pi$. This choice gives the uppermost limit for g under which perturbative techniques will be valid. The parameter Λ in Equation 1.1 is a mass scale which determines the strength of the coupling, but because this is a non-renormalizable interaction, it also characterizes the energy at which perturbative field theory techniques will break down. At energies below this scale, these perturbative techniques are perfectly acceptable and correspond to a Feynman vertex given in Figure 1.1. Following [7], a term like Equation 1.1 leads to the muon and the electron having a dipole moment, $\boldsymbol{\mu}$, of

$$\boldsymbol{\mu} = -\frac{g\eta}{\Lambda}\boldsymbol{\sigma} \tag{1.3}$$

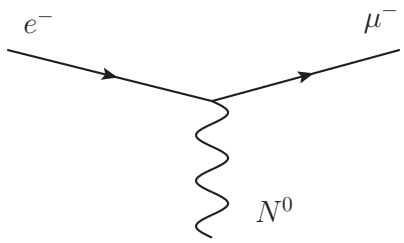

Figure 1.1: the Feynman vertex associated with the addition of Equation 1.1 to the Standard Model Lagrangian.

where the matrix $\boldsymbol{\sigma}$ is twice the spin of the lepton, and is given in terms of the Pauli matrices,

$$\begin{aligned} \boldsymbol{\sigma} &= (\sigma_1, \sigma_2, \sigma_3) \\ &= \left(\begin{bmatrix} 0 & 1 \\ 1 & 0 \end{bmatrix}, \begin{bmatrix} 0 & -i \\ i & 0 \end{bmatrix}, \begin{bmatrix} 1 & 0 \\ 0 & -1 \end{bmatrix} \right). \end{aligned} \tag{1.4}$$

We will consider several possible scenarios pertaining to this model, and we will obtain bounds for the parameters involved in each case by considering its contribution to a variety of measured processes including $e^+e^- \to \mu^+\mu^-$ and muonium-antimuonium oscillations.

The complete Lagrangian of interest is

$$\mathcal{L} = \mathcal{L}_{SM} + \mathcal{L}_{eff} + \mathcal{L}_{kin}, \tag{1.5}$$

where $\mathcal{L}_{SM}$ is the usual Standard Model Lagrangian and

$$\mathcal{L}_{kin} = -\frac{1}{4} N^{\mu\nu} N_{\mu\nu} \tag{1.6}$$

endows the gauge field N_μ with dynamics. In the following sections, we will justify this signature as a reasonable indicator of physics beyond the Standard Model.

1.1 Lepton Flavour Violation

The SM is a quantum field theory which contains the best tested quantitative description of the dynamics of quarks, leptons, and neutrinos, as well as the interactions of these particles via the electromagnetic, strong, and weak forces. It contains four distinct symmetries which are referred to as *global* symmetries, because they are the same at every point in space, and by Noether's Theorem

Decay Mode	Fraction $\frac{\Gamma_i}{\Gamma}$	Confidence
$\mu \to e^- + \gamma$	1.2×10^{-11}	90%
$\mu \to e^- + e^- + e^+$	1.0×10^{-12}	90%
$\mu \to e^- + 2\gamma$	7.2×10^{-11}	90%

Table 1.1: Constraints on lepton flavour violating modes of muon decay

these symmetries give rise to four distinct conserved quantities. These quantities are baryon number (B), electron lepton number (L_e), muon lepton number (L_μ), and tau lepton number (L_τ), and they are preserved by every process allowed by the SM in its current form. In addition, there is also the conservation of global lepton number; an immediate consequence of the three individual lepton number conservation laws. It should be noted, however, that unlike gauge symmetries, which appear to be a fundamental tool in the construction of physically realizable theories, these global symmetries seem to be accidental. This makes them easy targets in the search for physics beyond the SM. It turns out that the combination of baryon number and global lepton number conservation is extremely delicate due to the high constraints that have been placed on the decay of the proton [19], leaving us with only the individual U(1) lepton flavour symmetries with which to tinker. A large number of different LFV decays and processes have already been searched for and not found, placing some stringent experimental constraints on their parameters. Any model which seeks to include such processes must have mechanisms to account for their low abundance. Since our signature involves only couplings between muons and electrons, in Table 1.1 a few decay paths of particular interest and their experimental limits are shown as given by the Particle Data Group [19].

One interesting decay route is the decay of a muon into a photon and an electron, currently being searched for by the MEG experiment [1]. Such a process can become possible in a variety of SM extensions and is generally described by the effective interaction [20]

$$\mathcal{L}_{photon} = \frac{-4G_F}{\sqrt{2}}(m_\mu A_R \bar{\mu}_R \sigma^{\mu\nu} e_L F_{\mu\nu} + m_\mu A_L \bar{\mu}_L \sigma^{\mu\nu} e_R F_{\mu\nu} + H.C.) \tag{1.7}$$

which is of a strikingly similar form to our signature of interest, but without the addition of any non-SM fields. In this expression, A_R, A_L are model dependent coupling constants, G_F is the Fermi constant, and $F_{\mu\nu} = \partial_\mu A_\nu - \partial_\nu A_\mu$ is the gauge invariant electromagnetic field strength tensor. Often, as in this case, a given operator will contribute to more than one decay of interest. For example, this term also contributes to the decay of the muon into 3 electrons and, as we will discuss in Chapter 4, it is important that any such contributions are constrained to match the experimental bounds.

Recent experiments give strong evidence that neutrinos already violate flavour by oscillating between generations. Such processes are neutral LFV currents, but they also allow for charged

LFV processes to occur at the one loop level [25]. Neutrino masses, the expected source of these oscillations, are an open question in particle physics. Particularly, whether neutrinos are Dirac or Majorana fermions is unknown, and each has diferent effects on the conservation of the generational lepton numbers. In the Majorana case, not only are the individual generation numbers not conserved, but overall lepton number is no longer conserved either. Dirac masses also do not respect the three separate U(1) symmetries, but instead reduce them to a single conserved lepton number. Neutrino oscillations certainly further the case that lepton flavour is a window into structures beyond the SM. Just as quark flavour is violated by the weak interaction, and is beautifully described by the Cabibbo-Kobayashi-Masakawa matrix, it is not inconceivable that an as-yet-unseen gauge sector will violate lepton flavour.

1.2 Bosons Mediating Lepton Flavour Violation

The status of flavour violation in the leptonic sectors is a puzzling one; It is highly constrained by experimental searches, and yet it appears in a wide variety of extentions of the SM. While the particular mechanism involved in breaking generational lepton numbers in the charged sector varies drastically from theory to theory, in many of these models LFV occurs through interactions with new bosons. Here, we will discuss two extensions of the SM in which LFV is a result of as-yet-unseen bosonic interactions. For an overview of the interactions within the SM, the reader is directed to Appendix A.

One class of models that will be of interest are called 3-3-1 models. In these models, the gauge group of the SM is extended from $SU_C(3) \times SU_L(2) \times U_Y(1)$ to $SU_C(3) \times SU_L(3) \times U(1)$. The left-handed leptonic sector contains (l^-, ν_l, l^+) which transforms as a triplet under the new $SU_L(3)$ [10] gauge group. Because $SU(3)$ has eight generators, as opposed to three for $SU(2)$, this extension adds five gauge bosons to the electroweak sector. Four of these bosons are identifiable as *bileptons*; (X^{++}, X^+) carrying lepton number $L = -2$, and (X^{--}, X^-) carrying $L = 2$. These bosons acquire mass upon the spontaneous breaking of the leptonic $SU_L(3)$ gauge group. Their interactions with the lepton triplet is given by [11] as

$$\begin{aligned}\mathcal{L}_{int} = &-\frac{g_{3l}}{2\sqrt{2}} X_\mu^{++} l^T C\gamma^\mu\gamma_5 l - \frac{g_{3l}}{2\sqrt{2}} X_\mu^{--} l\gamma^\mu\gamma_5 C l^T \\ &+\frac{g_{3l}}{2\sqrt{2}} X_\mu^{+} l^T C\gamma^\mu(1-\gamma_5)\nu_l + \frac{g_{3l}}{2\sqrt{2}} X_\mu^{-} \bar{\nu}_l\gamma^\mu(1-\gamma_5) C l^T \end{aligned} \tag{1.8}$$

It should be noted that in this manifestation, the bileptons only interact in a flavour diagonal manner, mixing electrons with positrons, muons with antimuons, and so on. However, this need not be the case. In fact, the constraints on non-flavour diagonal interactions of bileptons have been found to be less constrained [24] than the flavour diagonal counterparts.

Another class of theories in which lepton flavour is broken by interactions with a boson are Left-Right Symmetric Models [23, 6]. In such theories, the electroweak sector of the SM is augmented to an $SU_L(2) \times SU_R(2) \times U_{B-L}(1)$ gauge symmetry. There are two sets of leptonic doublets, which are labeled in [23] as

$$\psi_L = \begin{pmatrix} \nu_L \\ \\ l_L \end{pmatrix} \quad , \quad \psi_R = \begin{pmatrix} \nu_R \\ \\ l_R \end{pmatrix}. \tag{1.9}$$

Let the generators of $SU_{L,R}(2)$ be denoted $T^i_{L,R}$ with $i = \{1, 2, 3\}$. The transformation properties of these doublets under these groups are given by the third component of each $SU(2)$ and their $B - L$ charge which we list as $(T^3_L, T^3_R, B - L)$. Then, the doublet ψ_L has $\left(\frac{1}{2}, 0, -1\right)$ and ψ_R has $\left(0, \frac{1}{2}, -1\right)$. The Higgs sector in this model needs to be much more elaborate, since now the symmetry between both the left- and right-handed sectors gets broken and all the leptons acquire mass. In minimal models, the Higgs sector is chosen to be [6] two-fold:

$$\phi = \begin{pmatrix} \phi^0_1 & \phi^+_1 \\ \\ \phi^-_2 & \phi^0_2 \end{pmatrix}, \tag{1.10}$$

a bidoublet whose vacuum expectation value endows the fermions with mass upon spontaneous symmetry breaking, and

$$\Delta_{L,R} = \begin{pmatrix} \frac{1}{\sqrt{2}}\Delta^+_{L,R} & \Delta^{++}_{L,R} \\ \\ \Delta^0_{L,R} & -\frac{1}{\sqrt{2}}\Delta^+_{L,R} \end{pmatrix}, \tag{1.11}$$

two additional bidoublets which break the left- and right-handed gauge symmetries. The most general Lagrangian for leptons under this symmetry is [23]

$$\begin{aligned} -\mathcal{L}_Y = f_{ij}\bar{\psi}^i_L \phi \psi^j_R + g_{ij}\bar{\psi}^i_L \tilde{\phi} \psi^j_R + H.C. \\ +h_{ij}\left(\psi^{iT}_L C\sigma_2 \Delta_L \psi^j_L + \psi^{iT}_R C\sigma_2 \Delta_R \psi^j_R\right) + H.C. \end{aligned} \tag{1.12}$$

where f and g are Yukawa coupling matrices. This Lagrangian leads to lepton flavour violation in two ways. First, it imbues the neutrinos with a Majorana mass (which we discuss in the previous section). Second, it turns out that the Higgs fields that we have written down also carry lepton

number of ± 2, and so can directly mediate LFV processes. In still more elaborate versions of this theory, like the one discussed in [21], a Goldstone boson called a *majoron* can emerge from an even larger Higgs sector, and mediate lepton flavour violating interactions at tree level.

Both of these classes of theories have been extensively studied in the literature, both as entities in their own right, and as the low energy effective theories for GUT scale models (See, for example, [10]), and much like many other models for physics beyond the SM, they contain lepton flavour violation as an almost immediate consequence of their structure.

1.3 the Dipole Operator

The dipole operator can be well understood in terms of the leptonic current decomposition, given by the Gordon Identity (proof in Appendix 1.A):

$$j^\mu = \bar{u}(k)\gamma^\mu u(p) = \frac{1}{2m}\bar{u}(k)(Q^\mu + i\sigma^{\mu\nu}q_\nu)u(p) \tag{1.13}$$

where $Q = (k + p)$ is the total momentum, $q = (k - p)$ is the momentum transfer and the dipole operator, $\sigma^{\mu\nu}$, is defined in Equation 1.2. Physically, this identity tells us that contained within the leptonic vector current is a dipole transition term. When we couple this equation to a electromagnetic source A_μ and take the non relativistic limit, we can expand our result in q and obtain

$$\bar{u}(k)\gamma^\mu u(p)A_\mu \approx A_0 - \frac{1}{2m}\left(\mathbf{Q}\cdot\mathbf{A} + i\boldsymbol{\sigma}\cdot(\mathbf{q}\times\mathbf{A})\right), \tag{1.14}$$

which is easily recognizable as having broken into electric and magnetic parts. It's clear from this decomposition that the dipole operator already plays a big part in our understanding of low energy physics.

In minimal extensions of the SM in which neutrinos are endowed with some small mass, it has been shown that dipole interactions allow for neutrinos to interact with light, despite their being neutrally charged under electromagnetism [7]. These interactions come about as a result of radiative loop corections to the neutrino propagator and can be accounted for by the term

$$\mathcal{L} = -\frac{1}{2}\mu\bar{\nu}\sigma^{\alpha\beta}\nu F_{\alpha\beta}, \tag{1.15}$$

where ν are the neutrino fields, μ is the neutrino magnetic dipole moment, and again $F_{\alpha\beta}$ is the electromagnetic field strength. The various diagrams encapsulated by this term are shown in Figure

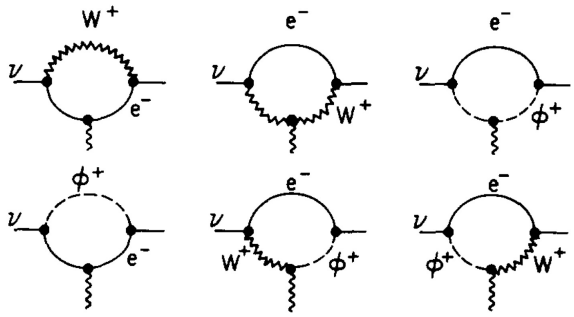

Figure 1.2: Radiative corrections to the neutrino propagator giving rise to a neutrino magnetic dipole moment. Here, ϕ^+ is the unphysical Higgs scalar [7].

1.2. There are several interesting situations to consider here. First, it is well known that a Majorana fermion is defined as a CPT self conjugate particle, and so is even under this transformation. Flavour diagonal dipole transitions, by contrast, are CPT-odd [14]. This means that a CPT invariant Lagrangian (or, because of the CPT Theorem, any local Lorentz invariant theory) cannot contain such a dipole transition. Neutrinos whose magnetic dipole moments are given by this term therefore must be Dirac fermions. The form of this operator also requires a change in chirality over the course of the transition. Consider starting with a left-handed neutrino:

$$\begin{aligned}
\mathcal{L} &= -\frac{1}{2}\mu\bar{\nu}\sigma^{\alpha\beta}\nu_L F_{\alpha\beta} \\
&= -\frac{1}{2}\mu\bar{\nu}\sigma^{\alpha\beta}P_L\nu F_{\alpha\beta} \\
&= -\frac{1}{2}\mu\bar{\nu}P_L\sigma^{\alpha\beta}\nu F_{\alpha\beta} \\
&= -\frac{1}{2}\mu\bar{\nu}_R\sigma^{\alpha\beta}\nu F_{\alpha\beta} \qquad (1.16)
\end{aligned}$$

So we must end up with a right-handed neutrino (For more details on chiral fermions and the projection operators, consult section 2.6) which is not contained in the SM (See Appendix A). The simplest scenario then, is to extend the SM to include a right-handed neutrino, which transforms as a singlet under the $SU_L(2)$ electroweak gauge group. Since only left handed neutrinos participate in gauge interactions, it is clear from the diagrams in Figure 1.2 that this chirality flip must occur on the external arm of the neutrino line, and so will be proportional to the neutrino mass. In fact, this dependence on the neutrino mass makes the resulting dipole moment about eight orders of magnitudes smaller than the current experimental bound [7]. Despite being small, the magnetic dipole moment of the neutrino clearly embodies a great deal of higher order physics. It seems natural then, to wonder about the possibility of higher order physics being hinted at by looking at similar interactions in the charged lepton sector as well.

1.A Appendix: Proof of the Gordon Identity

We can take the current

$$j^\mu = \bar{u}(k)\gamma^\mu u(p) \tag{1.17}$$

and break it up into

$$\frac{1}{2m}\bar{u}(k)(m\gamma^\mu + m\gamma^\mu)u(p). \tag{1.18}$$

We can then employ the Dirac equation for u and $\bar{u}$,

$$(\gamma^\nu p_\nu - m)u = 0 \tag{1.19}$$

$$\bar{u}(\gamma^\nu p_\nu - m) = 0, \tag{1.20}$$

to give

$$j^\mu = \frac{1}{2m}\bar{u}(k)(\gamma^\mu\gamma^\nu p_\nu + \gamma^\nu\gamma^\mu k_\nu)u(p). \tag{1.21}$$

We can use the anti-commutator of the gamma matrices

$$\{\gamma^\mu, \gamma^\nu\} = 2g^{\mu\nu}, \tag{1.22}$$

to obtain

$$\begin{aligned} j^\mu &= \frac{1}{2m}\bar{u}(k)[\gamma^\mu\gamma^\nu p_\nu + (2g^{\mu\nu} - \gamma^\mu\gamma^\nu)k_\nu]u(p) \\ &= \frac{1}{2m}\bar{u}(k)(2k^\mu - \gamma^\mu\gamma^\nu q_\nu)u(p), \end{aligned} \tag{1.23}$$

where we have defined $q = k - p$. Since 4-momentum is conserved, $q^\mu - k^\mu + p^\mu = 0$ and we can add 0 in this form to give

$$\begin{aligned} j^\mu &= \frac{1}{2m}\bar{u}(k)[k^\mu + p^\mu + (g^{\mu\nu} - \gamma^\mu\gamma^\nu)q_\nu]u(p) \\ &= \frac{1}{2m}\bar{u}(k)[Q^\mu + (g^{\mu\nu} - \gamma^\mu\gamma^\nu)q_\nu]u(p). \end{aligned} \tag{1.24}$$

Finally we consider the dipole operator

$$\begin{aligned} i\sigma^{\mu\nu} &= -\frac{1}{2}(\gamma^\mu\gamma^\nu - \gamma^\nu\gamma^\mu) \\ &= -\frac{1}{2}[\gamma^\mu\gamma^\nu - (2g^{\mu\nu} - \gamma^\mu\gamma^\nu)] \\ &= g^{\mu\nu} - \gamma^\mu\gamma^\nu, \end{aligned} \tag{1.25}$$

and thus

$$j^\mu = \bar{u}(k)\gamma^\mu u(p) = \frac{1}{2m}\bar{u}(k)[Q^\mu + \imath\sigma^{\mu\nu}q_\nu]u(p). \tag{1.26}$$

1.B Appendix: Proof of Electron Number Conservation in QED

Here we will show that electron number is indeed a conserved quantity in Quantum Electrodynamics (QED), and we will note that in the full SM after the breaking of the the electroweak symmetry, an analogous argument preserves muon number and tauon number. The Lagrangian density of QED can be written most succinctly as

$$\mathcal{L}_{QED} = \bar{\psi}(i\gamma^\mu D_\mu - m)\psi - \frac{1}{4}F^{\mu\nu}F_{\mu\nu}, \tag{1.27}$$

where we have written ψ as the electron field, $F^{\mu\nu} = \partial_\mu A_\nu - \partial_\nu A_\mu$ is the electromagnetic field strength tensor, and D_μ is the covariant derivative given by

$$D_\mu = \partial_\mu + ieA_\mu. \tag{1.28}$$

It is clear on inspection that this Lagrangian is invariant under the transformation

$$\psi \rightarrow e^{i\alpha}\psi, \tag{1.29}$$

where α is an arbitrary constant, independent of of the spacetime coordinates. To first order, this transformation can be written

$$\begin{aligned} \psi &\rightarrow \psi + \delta\psi \\ &= \psi + i\alpha\psi, \end{aligned} \tag{1.30}$$

and we will show that the current resulting form this U(1) symmetry is exactly the current which preserves electron number. The statement of invariance is equivalent to saying that the change in the Lagrangian, $\delta\mathcal{L}$, under this transformation of ψ must be zero, so we have

$$\begin{aligned} \delta\mathcal{L} &= \frac{\partial\mathcal{L}}{\partial\psi}\delta\psi + \frac{\partial\mathcal{L}}{\partial(\partial_\mu\psi)}\delta(\partial_\mu\psi) \\ &= \left(\frac{\partial\mathcal{L}}{\partial\psi} - \frac{\partial\mathcal{L}}{\partial(\partial_\mu\psi)}\right)\delta\psi + \partial_\mu\left(\frac{\partial\mathcal{L}}{\partial(\partial_\mu\psi)}\delta\psi\right), \end{aligned} \tag{1.31}$$

where the second step follows from integration by parts. Since this Lagrangian adheres to the principle of least action, it obeys the Euler-Lagrange equations of motion,

$$\frac{\partial\mathcal{L}}{\partial\psi} - \frac{\partial\mathcal{L}}{\partial(\partial_\mu\psi)} = 0, \tag{1.32}$$

leaving us with

$$\delta\mathcal{L} = \partial_\mu\left(\frac{\partial\mathcal{L}}{\partial(\partial_\mu\psi)}\delta\psi\right) = 0 \tag{1.33}$$

Substituting in, we are left with our statement of conserved current,

$$\partial_\mu(\bar{\psi}\gamma^\mu\psi) = 0. \tag{1.34}$$

Expanding the Lorentz indices of this current and rearranging, we have

$$\frac{d}{dt}\bar{\psi}\gamma^0\psi = \boldsymbol{\nabla}\cdot\bar{\psi}\boldsymbol{\gamma}\psi, \tag{1.35}$$

and upon integrating over space, and using the divergence theorem, where the fields go to zero at infinity, we have

$$\begin{aligned}\frac{d}{dt}\int J d^3x &= \frac{d}{dt}\int d^3x\ \bar{\psi}\gamma^0\psi \\ &= \frac{d}{dt}\int d^3x\ \psi^\dagger(\gamma^0)^2\psi \\ &= \frac{d}{dt}\int d^3x\ \psi^\dagger\psi = 0.\end{aligned} \tag{1.36}$$

We can expand J using the canonical expansion of the fermion fields

$$\begin{aligned}\psi &= \int \frac{d^3p}{(2\pi)^3}\frac{1}{\sqrt{2E_p}}\sum_s \left(a_p u(p)e^{-ip\cdot x} + b_p v(p)e^{ip\cdot x}\right) \\ \psi^\dagger &= \int \frac{d^3p}{(2\pi)^3}\frac{1}{\sqrt{2E_p}}\sum_s \left(a_p^\dagger u^\dagger(p)e^{ip\cdot x} + b_p^\dagger v^\dagger(p)e^{-ip\cdot x}\right),\end{aligned} \tag{1.37}$$

where we identify u, v as the spinors, $a, b^\dagger$ and $a^\dagger, b$ as annihilation and creation operators for electrons and positrons, respectively. The sum over s is a sum over the possible spin orientations for u and v. Plugging in, we get

$$\begin{aligned}J &= \int \frac{d^3p}{(2\pi)^3}\frac{1}{2E_p}\sum_s \left(a_p^\dagger u^\dagger(p)e^{ip\cdot x} + b_p^\dagger v^\dagger(p)e^{-ip\cdot x}\right)\left(a_p u(p)e^{-ip\cdot x} + b_p v(p)e^{ip\cdot x}\right) \\ &= \int \frac{d^3p}{(2\pi)^3}\frac{1}{2E_p}\sum_s \left(a_p^\dagger a_p u^\dagger(p)u(p) + b_p^\dagger b_p v^\dagger(p)v(p) + a_p^\dagger b_p u^\dagger(p)v(p)e^{2ip\cdot x} + b_p^\dagger a_p v^\dagger(p)u(p)e^{-2ip\cdot x}\right).\end{aligned} \tag{1.38}$$

Now we can use the orthogonality relations of the spinors u, v to simplify this expression. Both u and v can take on spin up, or spin down, and we denote these choices by $u_\pm(p)$ and $v_\pm(p)$. Then, our relations are

$$\begin{aligned} u_{\pm}^{\dagger}(p)u_{\pm}(p) = v_{\pm}^{\dagger}(p)v_{\pm}(p) = E_p \\ u_{\pm}^{\dagger}(p)u_{\mp}(p) = v_{\pm}^{\dagger}(p)v_{\mp}(p) = 0 \\ u_{\pm}^{\dagger}(p)v_{\pm}(p) = v_{\pm}^{\dagger}(p)u_{\pm}(p) = 0 \\ u_{\pm}^{\dagger}(p)v_{\mp}(p) = v_{\pm}^{\dagger}(p)u_{\mp}(p) = 0. \end{aligned} \tag{1.39}$$

This allows us to write J as

$$\begin{aligned} J &= \int \frac{d^3p}{(2\pi)^3}\frac{1}{2E_p}\left(a_p^{\dagger}a_p(E_p+E_p) + b_p^{\dagger}b_p(E_p+E_p)\right) \\ &= \int \frac{d^3p}{(2\pi)^3}\left(a_p^{\dagger}a_p + b_p^{\dagger}b_p\right). \end{aligned} \tag{1.40}$$

What does this operator tell us? Suppose we have a system with n electrons and n positrons. Then this operator will annihilate a positron with momentum p for every one it creates, and create an electron with momentum p for one it annihilates. Assigning electrons an electron number of $+1$ and positrons an electron number of -1, this operator counts electron number locally, or at each point in spacetime. Because we have that

$$\frac{d}{dt}\int J\ d^3x = 0, \tag{1.41}$$

it is clear that this number L_e is conserved for all process. In the SM, at energies below the scale of electroweak symmetry breaking, each of the charged lepton generations end up with a Lagrangian density analogous to Equation 1.27, and so the conservation of each individual lepton number follows from an almost identical analysis as this.

It is important to note that because of the use the classical equation of motion, Equation 1.32, this is a strictly classical proof, which is to say that we have only proven electron number conservation for tree level processes. While quantum mechanics is, in general, capable of breaking symmetries which hold at tree level (called *anomalies*), it is a non trivial point that in this case, it does not. For details on anomalies within the SM, the reader is directed to [26].

Chapter 2

Constraints from $e^+e^- \to \mu^+\mu^-$

2.1 The Cross Section

In the SM, there are only two diagrams at tree level for the process $e^+e^- \to \mu^+\mu^-$: by the photon, and by the Z boson. These are shown in Figure 2.1.

The addition of our signature induces a third mechanism for the process to occur, via our neutral N^0 boson, and this process is shown in Figure 2.2. Each of these diagrams is associated with an matrix element which we denote $\mathcal{M}$, obtained by the application of the Feynman rules (See Appendix 2.A). In a typical experimental set up, such as that at LEP, we would be concerned with unpolarized electron beams, and so we would want to average over the initial spins and sum over the final spins of our particles of interest. However, even if the beams were polarized, we would simply use projections operators (described in Section 2.6), and we would average and sum in the same fashion. We will obtain the spin averaged square of our amplitudes, and denote them generally by

$$\langle|\mathcal{M}|^2\rangle = \frac{1}{4}\sum_{spins}|\mathcal{M}|^2 \tag{2.1}$$

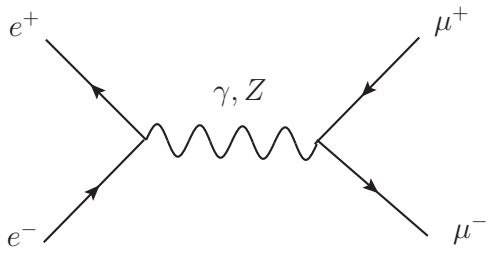

Figure 2.1: Tree level processes for $e^+e^- \to \mu^+\mu^-$ in the Standard Model. The γ indicates an intermediate photon, while the Z indicates an intermediate Z boson.

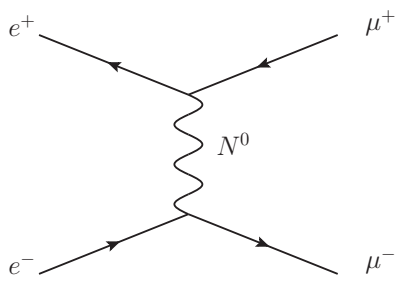

Figure 2.2: The contribution from the N^0 boson to the process $e^+e^- \to \mu^+\mu^-$

The factor of four comes from the fact that that each of incoming electron beams could have either spin up or spin down, giving a total of 4 possibilities to be averaged over. The amplitudes for the SM processes are given below

$$\mathcal{M}_\gamma = \left(\frac{e^2}{k^2}\right)\bar{v}(p_2)\gamma^\mu u(p_1)\bar{u}(p_4)\gamma_\mu v(p_3) \tag{2.2}$$

$$\mathcal{M}_Z = C_Z\bar{v}(p_2)\gamma^\sigma(C_V - \gamma^5 C_A)u(p_1)\left(g_{\nu\sigma} - \frac{k_\nu k_\sigma}{m_Z^2}\right)\bar{u}(p_4)\gamma^\nu(C_V - \gamma^5 C_A)v(p_3) \tag{2.3}$$

where u and v are the spinors. We have taken the conventional labeling scheme of p_1 being the momentum of the incoming electron, p_2 being the momentum of the incoming positron, p_3 being the momentum of the outgoing muon, and p_4 being the momentum of the outgoing antimuon. We will also use the convention that

$$k^\mu = (p_1^\mu + p_2^\mu) \tag{2.4}$$

$$q^\mu = (p_1^\mu - p_3^\mu) \tag{2.5}$$

from here on, unless otherwise noted. For further details on the kinematic choices, see Appendix 2.B. In Equation 2.2, C_Z contains the relevant coupling constants and the propagator denominator with the mass and decay width of the Z boson labeled respectively as m_Z and Γ_Z,

$$C_Z = \frac{e^2}{4c_W^2 s_W^2(k^2 - m_Z^2 + im_Z\Gamma_Z)}. \tag{2.6}$$

We denote

$$c_W = \cos\theta_W \tag{2.7}$$
$$s_W = \sin\theta_W \tag{2.8}$$

being functions of the Weinberg angle (see Appendix A) and, for leptons, the coefficients C_A and C_V are known to be

$$C_A = -\frac{1}{2} \tag{2.9}$$
$$C_V = -\frac{1}{2} + 2s_W^2. \tag{2.10}$$

Following the Feynman rules for our signature, we obtain the amplitude for the contribution from the N^0,

$$\mathcal{M}_N = C_N q_\alpha q_\beta \bar{v}(p_2)\sigma^{\delta\alpha}v(p_3)\left(g_{\delta\lambda} - \frac{q_\delta q_\lambda}{m_N^2}\right)\bar{u}(p_4)\sigma^{\lambda\beta}u(p_1), \tag{2.11}$$

where, analogously, the coupling and propagator denominator have been absorbed into

$$C_N = \frac{4\pi}{\Lambda^2(q^2 - m_N^2 + im_N\Gamma_N)}, \tag{2.12}$$

and we have labeled the mass of our new particle by m_N, it's decay width by Γ_N, and the mass-scale of the Lagrangian operator by Λ.

We will need to compute the cross section, σ, for this process, as we will compare our model to the existing measurements in order to obtain bounds for m_N and Λ. As details of these calculations are left for Appendices 2.A and 2.B, we will simply state the results of the computations here. We will require the quantity

$$\begin{aligned}\langle|\mathcal{M}|^2\rangle &= \langle|\mathcal{M}_\gamma + \mathcal{M}_z + \mathcal{M}_N|^2\rangle \\ &= \langle|\mathcal{M}_\gamma + \mathcal{M}_z|^2\rangle + \langle|\mathcal{M}_N|^2\rangle + \langle\mathcal{M}_{N,\gamma}\rangle + \langle\mathcal{M}_{N,Z}\rangle,\end{aligned} \tag{2.13}$$

where we have labeled the two terms corresponding to the interference of the N^0 boson with the SM processes as

$$\begin{aligned} \langle \mathcal{M}_{N,\gamma} \rangle &= \langle \mathcal{M}_{\gamma}^{*} \mathcal{M}_{N} \rangle + \langle \mathcal{M}_{\gamma} \mathcal{M}_{N}^{*} \rangle \\ \langle \mathcal{M}_{N,Z} \rangle &= \langle \mathcal{M}_{Z}^{*} \mathcal{M}_{N} \rangle + \langle \mathcal{M}_{Z} \mathcal{M}_{N}^{*} \rangle \end{aligned} \tag{2.14}$$

We will reproduce the tree level results for the SM, $\langle |\mathcal{M}_{\gamma} + \mathcal{M}_{z}|^2 \rangle$, for two reasons: to ensure that our methodology is sound, and to investigate the accuracy of the tree level processes compared with the results from the analytical program Zfitter [2]. There will be three contributions to this: the photonic, the neutral weak, and the interference part, which we will label $\langle |\mathcal{M}_{\gamma}|^2 \rangle$, $\langle |\mathcal{M}_{Z}|^2 \rangle$, and $\langle \mathcal{M}_{I} \rangle$ where

$$\langle \mathcal{M}_{I} \rangle = \langle \mathcal{M}_{\gamma}^{*} \mathcal{M}_{Z} \rangle + \langle \mathcal{M}_{\gamma} \mathcal{M}_{Z}^{*} \rangle \tag{2.15}$$

and we will state here the resulting differential cross sections, leaving the details of the calculations for Appendix 2.A.

Since the data we will be using comes from collider experiments, we will express our cross sections in terms of quantities which are relevant to the experimental set up. In the Center of Mass frame, let E be the energy of each of the incoming particles, and let θ be the angle between the momenta p_1 and p_3 (see Appendix 2.B). The differential cross section for two-body to two-body scattering is given by [22]

$$\frac{d\sigma}{dcos\theta} = \left(\frac{(2\pi)\sqrt{E^2 - m_{\mu}^2}}{64(2\pi)^2 E^3} \right) \langle |\mathcal{M}_{\gamma}|^2 + |\mathcal{M}_{z}|^2 + \mathcal{M}_{I} \rangle. \tag{2.16}$$

A Mathematica package called TwoToTwo was developed and used for the evaluation of the different contributions, and we cite the results below in terms of kinematic variables. We obtain, for the photonic process,

$$\frac{d\sigma_{\gamma}}{dcos\theta} = \frac{\pi\alpha^2}{8E^2} \sqrt{1 - \frac{m_{\mu}^2}{E^2}} \left[\left(1 + \frac{m_e^2 + m_{\mu}^2}{E^2} \right) + \cos^2\theta \left(\frac{m_{\mu}^2}{E^2} - 1 \right) \left(\frac{m_e^2}{E^2} - 1 \right) \right], \tag{2.17}$$

for the neutral weak process, we have

$$\begin{aligned}\frac{d\sigma_Z}{dcos\theta} &= \frac{\pi\alpha^2 E^2\sqrt{1-\frac{m_\mu^2}{E^2}}}{8s_W^4 c_W^4[(4E^2-m_z^2)^2+m_z^2\Gamma_z^2]}\left((1+\cos^2\theta)\left[(C_A^2+C_V^2)^2-\frac{m_e^2+m_\mu^2}{E^2}(C_A^4-C_V^2C_A^2)\right]\right.\\ &+ \sin^2\theta\left(\frac{m_e^2+m_\mu^2}{E^2}\right)(C_V^4+C_A^2C_V^2)-8C_A^2C_V^2\cos\theta\sqrt{\left(1-\frac{m_\mu^2}{E^2}\right)\left(1-\frac{m_e^2}{E^2}\right)}\\ &+ \left.\frac{m_e^2m_\mu^2}{E^4}\left[C_A^4(2+\cos^2\theta)-2C_A^2C_V^2\sin^2\theta+C_V^4\cos^2\theta+\frac{16C_A^4E^2}{m_Z^2}\left(\frac{E^2}{m_Z^2}-\frac{1}{2}\right)\right]\right), \quad (2.18)\end{aligned}$$

and the contribution from both interference terms, designated here by I, are

$$\begin{aligned}\frac{d\sigma_{\rm I}}{d\cos\theta} &= \frac{\pi\alpha^2\sqrt{1-\frac{m_\mu^2}{E^2}}(4E^2-m_z^2)}{4c_W^2s_W^2[(4E^2-m_z^2)^2+m_z^2\Gamma_z^2]}\left((1+\cos^2\theta)C_V^2+\sin^2\theta C_V^2\left(\frac{m_e^2+m_\mu^2}{E^2}\right)\right.\\ &+ \left.\cos^2\theta\left(\frac{m_e^2m_\mu^2C_V^2}{E^4}\right)-2\cos\theta\sqrt{(1-\frac{m_e^2}{E^2})(1-\frac{m_\mu^2}{E^2})}\right). \quad (2.19)\end{aligned}$$

These are written in such a way that, upon setting $m_e = 0$, the result can quickly be compared with the results from the program ZFitter [2]. The total differential cross section is then given by the sum of these contributions,

$$\frac{d\sigma_{\rm tot}}{d\cos\theta} = \frac{d\sigma_{\rm Z}}{d\cos\theta} + \frac{d\sigma_\gamma}{d\cos\theta} + \frac{d\sigma_{\rm I}}{d\cos\theta} \quad (2.20)$$

and the total SM cross section can then be obtained by integration

$$\sigma_{SM} = \int_{-0.94}^{0.94}\left(\frac{d\sigma_{\rm Z}}{d\cos\theta} + \frac{d\sigma_\gamma}{d\cos\theta} + \frac{d\sigma_{\rm I}}{d\cos\theta}\right)d\cos\theta \quad (2.21)$$

and compared with the data from the LEP experiments [16], to investigate the accuracy of the tree-level processes. The total cross section is defined as the differential cross section integrated from $[-1, 1]$, and the choice to integrate it from $[-0.94, 0.94]$ is indicative of the reality that the experimental set up is incapable of measuring events that occur within a small range of angles, close to where to beams are positioned. These limits of integration are the most conservative limits taken from the DELPHI experiment at LEP [16]. Figure 2.3 illustrates the measurement of the total cross section for three different processes: $e^+e^- \to \mu^+\mu^-, \tau^+\tau^-$, and hadrons. These cross sections are measured at various energies and are shown plotted with the solid black lines, which are the theoretical curves generated by Zfitter. The addition of the N^0 will generate distortions in

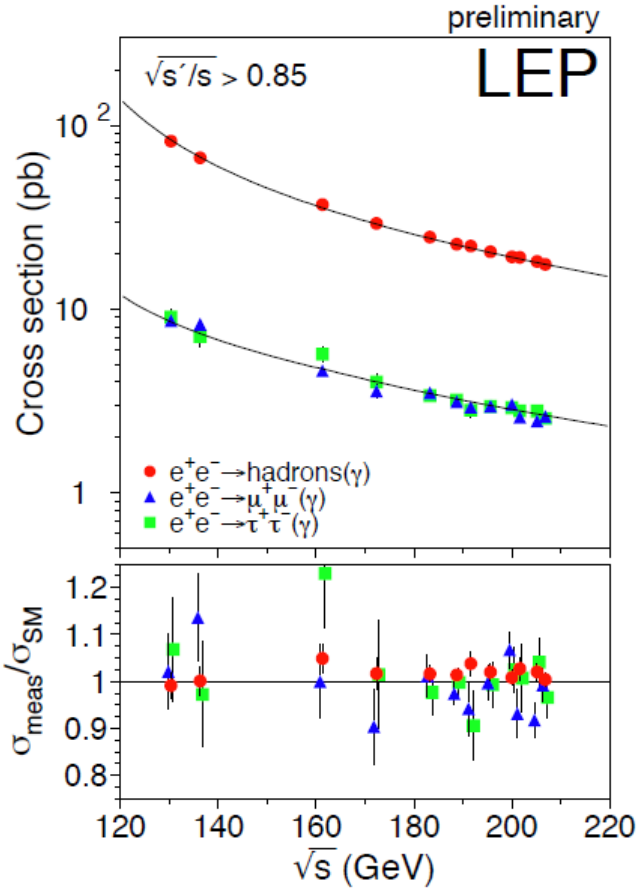

Figure 2.3: A reproduction of Figure 2 from [16]. Cross Sections for $e^+e^- \to \mu^+\mu^-$, in picobarnes above, and as a fraction of the SM prediction below, are shown in blue plotted against the center-of-mass energy $\sqrt{s}$. The black line is the theoretical prediction from Zfitter.

this curve, based on the values chosen for the various parameters. Requiring that these distortions maintain a strong fit with the data will allow us to place constraints on the possible values these parameters can take.

The interference of the hypothetical N^0 particle with the SM processes will in principle be dependent on the parameters Λ, m_N, and Γ_N, and the distortions mentioned before will occur by varying the values of these parameters. We will be interested in two different scenarios: a very heavy mediator, and a very light mediator.

2.2 Heavy Mediator

If the N^0 boson is sufficiently heavy, we can make a few good approximations. First, in any energy regime where N^0 is relevant, the masses of the leptons are negligible, so we will drop them. Second, the assumption of a heavy mediator also allows us to simplify its propagator. In the unitary gauge [4], the exact propagator of the N^0 with momentum q_μ is

$$\Pi_{\mu\nu} = \frac{-i(g_{\mu\nu} - \frac{q_\mu q_\nu}{m_N^2})}{q^2 - m_N^2 + i m_N \Gamma_N}, \tag{2.22}$$

but with m_N very large we can safely make two approximations:

$$\begin{aligned} \frac{\Gamma_N}{m_N} &<< 1, \\ \frac{t}{m_N^2} &<< 1, \end{aligned} \tag{2.23}$$

where $t = q_\mu q^\mu = q^2$ is the Mandelstam variable corresponding to the momentum transfer. These approximations leave us with the simplified propagator

$$\Pi_{\mu\nu} = \frac{i}{m_N^2}(g_{\mu\nu} - \frac{q_\mu q_\nu}{m_N^2}) \tag{2.24}$$

which is the mathematical statement that we are treating our interaction as a contact interaction that has no dispersion through space. We could, in principle, also drop the numerator term $q_\mu q_\nu m_N^{-2}$, but because of the antisymmetric structure of $\sigma^{\mu\nu}$, these terms are exactly zero anyways. Upon evaluating $\langle \mathcal{M}_{N,\gamma} \rangle$, $\langle \mathcal{M}_{N,Z} \rangle$, and $\langle \mathcal{M}_N^2 \rangle$ with the simplifications made above, we obtain our lepton flavour violating contributions to the differential cross section:

$$\frac{d\sigma_{N,\gamma}}{d\cos\theta} = \frac{\pi\alpha E^2}{2\Lambda^2 m_N^2}(1-\cos\theta)^2(\cos\theta+3), \tag{2.25}$$

for the photon,

$$\frac{d\sigma_{N,Z}}{d\cos\theta} = \frac{\alpha E^4(C_A^2-C_V^2)(4E^2-m_Z^2)(1-\cos\theta)^2(\cos\theta+3)}{2c_W^2 s_W^2\Lambda^2 m_N^2[(4E^2-m_Z^2)^2+m_Z^2\Gamma_Z^2]}, \tag{2.26}$$

for the Z boson, and

$$\frac{d\sigma_{N,N}}{d\cos\theta} = \frac{2\pi E^6}{\Lambda^4 m_N^4}(1-\cos\theta)^2(\cos\theta+3)^2 \tag{2.27}$$

from the N^0 amplitude squared. Just as with the electroweak differential cross sections, the total contribution from our signature is given by

$$\sigma_N = \int_{-0.94}^{0.94}\left(\frac{d\sigma_{N,Z}}{d\cos\theta}+\frac{d\sigma_{N,\gamma}}{d\cos\theta}+\frac{d\sigma_{N,N}}{d\cos\theta}\right)d\cos\theta \tag{2.28}$$

such that it can be added to σ_{SM} and compared with the data from LEP2.

2.3 Light Mediator

There is another possibility worth considering, which is that rather than being very heavy, the N^0 particle is very light, and has not been observed due to the weakness of its interactions with known particles. In this case, we assume

$$\frac{m_N^2}{t} << 1 \tag{2.29}$$

and so our modified propagator will be

$$\Pi_{\mu\nu} = \frac{-i}{t}(g_{\mu\nu}-\frac{q_\mu q_\nu}{m_N^2}) \tag{2.30}$$

Since the mediator is now light, it is not necessarily true that the masses of leptons will be negligible in any process that this interaction contributes to. It is worth emphasizing though, that

this is a non-renormalizable interaction and so it has an energy scale Λ associated with it. If Λ were on the same order as the masses of the leptons, this interaction would have already been apparent in scattering experiments. Since this is not the case, it is clear that any scattering event in which the N^0 could be detected must be energetic enough to safely neglect the mases of the leptons. In this regime, the differential cross sections are

$$\frac{d\sigma_{N,\gamma}}{d\cos\theta} = -\frac{\pi\alpha}{\Lambda^2}(1-\cos\theta)(\cos\theta+3) \tag{2.31}$$

for the photon,

$$\frac{d\sigma_{N,Z}}{d\cos\theta} = \frac{\pi\alpha E^2(C_V^2-C_A^2)(4E^2-m_Z^2)}{4c_W^2 s_W^2\Lambda^2[(4E^2-m_Z^2)^2+m_Z^2\Gamma_Z^2]}(1-\cos\theta)(\cos\theta+3) \tag{2.32}$$

for the Z boson, and

$$\frac{d\sigma_{N,N}}{d\cos\theta} = \frac{\pi E^2}{2\Lambda^4}(\cos\theta+3)^2 \tag{2.33}$$

for the N^0 amplitude squared. Just as before the total cross section is obtained by integration:

$$\sigma_N = \int_{-0.94}^{0.94}\left(\frac{d\sigma_{N,Z}}{d\cos\theta}+\frac{d\sigma_{N,\gamma}}{d\cos\theta}+\frac{d\sigma_{N,N}}{d\cos\theta}\right)d\cos\theta \tag{2.34}$$

and compared with the data from LEP.

2.4 The Forward-Backward Asymmetry

Another quantity which has been measured in scattering experiments is the forward-backward asymmetry, A_{FB}. Let us suppose that the differential cross section contains some part that goes like $\cos\theta$ for a given scattering process. Upon integration to obtain the full cross section, σ, this part will be zero. The forward-backward asymmetry is a quantity which can capture the contribution to the scattering by this piece of the differential cross section. Physically, if we are looking at, for example, $e^+e^- \to \mu^+\mu^-$, the forward-backward asymmetry is the difference between the number of muons scattered forward versus the number of muons scattered backwards with respect to the electron beam line. Before we define it explicitly, it is worth noting that one of the reasons that A_{FB} is a force to be contended with is that the SM inherently violates parity, a symmetry long held sacred in physical theories. In the case of processes like the one we are interested in, where a particle-antiparticle pair

E_{CM}	A_{FB}^{SM}	Measured A_{FB} (LEP)
130 GeV	0.684	0.694 ± 0.060
136 GeV	0.664	0.708 ± 0.060
161 GeV	0.600	0.538 ± 0.067
172 GeV	0.581	0.675 ± 0.077
183 GeV	0.566	0.559 ± 0.035
189 GeV	0.558	0.569 ± 0.021

Table 2.1: Comparison of the tree level calculation of the Standard Model A_{FB} with the measured values obtained at LEP at the lowest six energies. The measured values are taken from Table 2 in [16], and values in the second column were calculated using equation 2.36. Here, E_{CM} is the center of mass energy.

are produced, the statement that the differential cross section goes like $\cos\theta$ means that the resulting pairs of particles preferentially choose the direction they will end up moving in upon creation. In the SM, this behaviour comes in part from the fact that the weak interaction violates parity in its differing treatment of right-handed and left-handed fermions. Even in a parity-conserving theory however (like quantum electrodynamics), loop corrections can induce a non-zero A_{FB}. With all of this in mind, we define the forward-backward asymmetry as the ratio [22],

$$A_{FB} = \frac{\int_0^{0.94} \frac{d\sigma}{d\cos\theta} d\cos\theta - \int_{-0.94}^{0} \frac{d\sigma}{d\cos\theta} d\cos\theta}{\sigma_{tot}} \tag{2.35}$$

Again, the total forward-backward asymmetry would be integrated from 0 to 1 and -1 respectively, but in keeping with the conventions from scattering, we will restrict our integration to the measurable regions. The forward-backward asymmetry for muon pair production was computed for the SM at tree level to investigate the degree of agreement with the data, and the result is

$$A_{FB}^{SM} = \frac{C_A^2 E^2 (7.07 C_V^2 E^2 + c_W^2 s_W^2 (14.14E^2 - 3.5 m_Z^2))}{f(E)}, \tag{2.36}$$

where

$$\begin{aligned} f(E) = {} & E^4(2.43C_A^4 + 4.87C_A^2C_V^2 + 2.43C_V^4 + 19.47C_V^2c_W^2s_W^2 + 38.94c_W^4s_W^4) - \\ & E^2m_Z^2(4.87C_V^2c_W^2s_W^2 + 19.47c_W^4s_W^4) + c_W^4s_W^4(2.43m_Z^4 + 2.43m_Z^2\Gamma_Z^2) \end{aligned} \tag{2.37}$$

where again, we have defined $E = \frac{1}{2}E_{CM}$ being the energy of each incoming beam. Table 2.1 shows

the agreement of the tree level calculation with the measured values from LEP for the smallest six energies.

For each of the two scenarios, we can reparametrize the dependence on the N^0 mass and coupling using a variable which we will call ϵ. We can then build the forward-backward asymmetry as a function of ϵ and what we end up with schematically looks like

$$A_{FB}(E,\epsilon) = \frac{1}{\sigma_{SM} + \sigma_{N^0}(\epsilon)} \left(\int_0^{0.94} \left(\frac{d\sigma_{SM}}{d\cos\theta} + \frac{d\sigma_{N^0}(\epsilon)}{d\cos\theta} \right) d\cos\theta - \int_{-0.94}^{0} \left(\frac{d\sigma_{SM}}{d\cos\theta} + \frac{d\sigma_{N^0}(\epsilon)}{d\cos\theta} \right) d\cos\theta \right) \tag{2.38}$$

As these expressions become extremely complicated, even in the limit of massless fermions, we will omit them from this section, but include the results in Appendix 2.C for reference.

2.5 Fits and Results

In both the heavy and light mediator scenarios, the parameter ϵ was used for the fits, with

$$\epsilon_H \equiv \frac{1}{\Lambda^2 m_N^2} \tag{2.39}$$

for the heavy case and

$$\epsilon_L \equiv \frac{1}{\Lambda^2} \tag{2.40}$$

for the light case, and was allowed to take on both positive and negative values with $\epsilon > 0$ corresponding to $\eta = +1$ and $\epsilon < 0$ corresponding to $\eta = -1$ in our signature.

To obtain the central values for ϵ, the method of Maximum Likelihood [3, 17] was used, which we will briefly discuss. Suppose we have obtained N measurements $\{x_i\}$ of a physical quantity x, each of which is obtained from a probability distribution function $f(x|\lambda)$ and λ is some unknown parameter. The probability distribution function is interpreted here as the probability density of measuring x_i given λ. However, if we do not know λ, we wish to choose its value such that there is optimal correspondence with the set of observations. Very generally, we define the likelihood function as [3]

$$L(\lambda) = \prod_{i=1}^{N} f(x_i|\lambda), \tag{2.41}$$

which tells us the probability density of finding the entire set of observations $\{x_i\}$ [17]. To obtain

the *maximum likelihood estimate* for λ, we must maximize $L(\lambda)$,

$$\frac{dL(\lambda)}{d\lambda} = 0, \tag{2.42}$$

and the solution which satisfies this equation will be our best estimate. In the event that the probability distribution function $f(x|\lambda)$ is well approximated by a normal distribution, as is the case for the measurements obtained at LEP, we may define our likelihood function, L, as

$$L = e^{-\frac{1}{2}\chi^2}, \tag{2.43}$$

where the χ^2 is defined separately for the cross section and for the forward-backward asymmetry. For the cross section, it is defined as

$$\chi^2_\sigma = \sum_i \left(\frac{\sigma_{meas}(E_i) - \sigma_{th}(E_i, \epsilon)}{\delta\sigma_{meas}(E_i)} \right)^2. \tag{2.44}$$

Here, the sum is over individual measurements with E_i representing the energy at which that measurement was made. The quantity σ_{meas} is the cross section actually measured by LEP, σ_{th} is the theoretical cross section, which amounts to the SM cross section plus the contribution from the LFV signature, and $\delta\sigma_{meas}(E_i)$ is the error in the measurement of σ_{meas}. For the forward-backward asymmetry, we analogously define

$$\chi^2_{AFB} = \sum_i \left(\frac{A^{meas}_{FB}(E_i) - A^{th}_{FB}(E_i, \epsilon)}{\delta A^{meas}_{FB}(E_i)} \right)^2, \tag{2.45}$$

with $A^{meas}_{FB}(E_i)$ and $A^{th}_{FB}(E_i, \epsilon)$ being the measured and theoretical forward-backward asymmetries respectively. Once these likelihood functions were constructed, they were each maximized to obtain the central value for ϵ. We define the one standard deviation, or 1σ, error range as the limits where the likelihood function is reduced by its maximum value by a factor of $e^{\frac{1}{2}}$. By this definition, it is clear why the we can leave the Likelihood unnormalized: we are solving

$$L(\epsilon) = e^{-\frac{1}{2}} L_{max}, \tag{2.46}$$

and any normalization factor included would be common to both sides. Probabilistically, the meaning of this is that there is a 68.2% chance of of finding the 'true' value of ϵ within the range stated.

The separate results from each of these analyses were then combined by way of a weighted mean, defined as

$$\bar{\epsilon} = \sum_i \epsilon_i w_i \tag{2.47}$$

with the weights, w_i given by

$$w_i = \frac{1}{\delta\epsilon_i^2} \tag{2.48}$$

The error on this value, which we call $\delta\bar{\epsilon}$, was then obtained using the formula

$$\frac{1}{\delta\bar{\epsilon}^2} = \sum_i \frac{1}{\delta\epsilon_i^2} \tag{2.49}$$

The values given by these fits for both the heavy and light mediator cases are given in Table 2.2. In addition to these central values, 95% confidence limits could also be placed on the parameter ϵ for $\eta = \pm 1$. Physically, this confidence limit tells us that if we did 100 experiments, 95 of those those experiments would yield a bound on ϵ of equal or lesser strength. To obtain these limits one must normalize the Likelihood function over the physically allowed values of ϵ. We define

$$\begin{aligned} N_+ &= \int_0^\infty L(\epsilon)\ d\epsilon \\ N_- &= \int_{-\infty}^0 L(\epsilon)\ d\epsilon \end{aligned} \tag{2.50}$$

and now we can define the normalized Likelihood functions for $\eta = +1$ and $\eta = -1$ respectively as

$$L_\pm(\epsilon) = \frac{1}{N_\pm} L(\epsilon). \tag{2.51}$$

To obtain the 95% limits on ϵ, we integrate the normalized likelihood functions up to a point which we refer to as $\epsilon^\star$ and set that integral equal to 0.95. Explicitly, for $\eta = \pm 1$, we numerically evaluate

Model	ϵ from σ	ϵ from A_{FB}	Weighted Mean, $\bar{\epsilon}$
Heavy N^0 (TeV^{-4})	$-0.3879^{+0.2672}_{-0.3170}$	$-0.0911^{+0.1651}_{-0.1632}$	-0.1623 ± 0.1431
Light N^0 (TeV^{-2})	$-0.0096^{+0.0069}_{-0.0103}$	$-0.0030^{+0.0052}_{-0.0052}$	-0.0048 ± 0.0044

Table 2.2: Central values for ϵ found by maximizing the Likelihood function in both the heavy and light N^0 scenarios. Independent values were found using data from the measurements of the cross section, σ, and the forward-backward asymmetry, A_{FB}. These two values were then combined in a weighted average, $\bar{\epsilon}$.

Model	$(\epsilon^\star_+)^{-\frac{1}{2}}$ from σ	$(\epsilon^\star_-)^{-\frac{1}{2}}$ from σ	$(\epsilon^\star_+)^{-\frac{1}{2}}$ from A_{FB}	$(\epsilon^\star_-)^{-\frac{1}{2}}$ from A_{FB}
Heavy N^0, $(\Lambda m_N)^\pm$	2.0 TeV^2	0.3 TeV^2	1.9 TeV^2	1.6 TeV^2
Light N^0, $\Lambda^\pm$	13.0 TeV	4.0 TeV	10.7 TeV	9.1 TeV

Table 2.3: 95% Confidence Limits for Λ and Λm_N obtained from fits to the cross section, σ, and the forward-backward asymmetry, A_{FB}. These values correspond to a choice of $\eta = \pm 1$ for each of the two sets of measurements, with $\epsilon^\star_+$ corresponding to a choice of $\eta = 1$ and $\epsilon^\star_-$ corresponding to a choice of $\eta = -1$.

$$\int_0^{\epsilon^\star_+} L_+(\epsilon)d\epsilon = 0.95$$
$$\int_{-\epsilon^\star_-}^{0} L_-(\epsilon)d\epsilon = 0.95 \tag{2.52}$$

for the limits $\epsilon^\star_+$ and $\epsilon^\star_-$. This process was done for the fits from both the cross section and the forward-backward asymmetry analyses, and the results for both the heavy and light N^0 cases are presented in Table 2.3. It is worth noting that the normalization of the likelihood function for $\eta = \pm 1$ turns it into a probability density function, and that the integration over the physically allowed values of ϵ is equivalent to multiplying $L(\epsilon)$ by a uniform prior probability function in ϵ [16].

2.6 Comparison with Four-Fermion Constraints

In order to gain confidence and check our statistical methods, we reproduced the constraints put on a variety of four-fermion lepton flavour violating signatures that were obtained by the research group at LEP [16]. Following the conventions of [8], the signatures emerge from an effective Lagrangian of the form

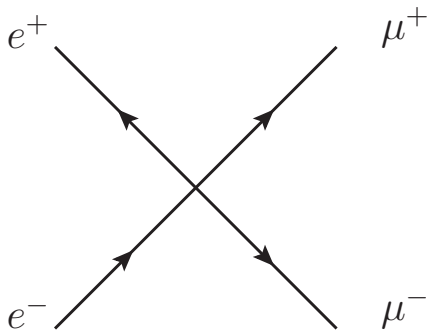

Figure 2.4: This is the only tree level diagram which contributes to $e^+e^- \to \mu^+\mu^-$ from the 4-fermion operators looked at by LEP [16].

$$\mathcal{L}_{eff} = \frac{g^2}{\Lambda^2}\eta_{ij}\bar{e}_i\gamma_\mu e_i\bar{\mu}_j\gamma^\mu\mu_j, \tag{2.53}$$

where i,j = L,R standing for left and right handed fermions, $\eta = \pm 1$, and again we take $g^2 = 4\pi$. Two models which do not obviously follow this labeling scheme but were also investigated are the Vector-Vector interaction:

$$\mathcal{L}_{eff} = \frac{g^2}{\Lambda^2}\eta\bar{e}\gamma_\mu e\bar{\mu}\gamma^\mu\mu, \tag{2.54}$$

and the Axial-Axial interaction:

$$\mathcal{L}_{eff} = \frac{g^2}{\Lambda^2}\eta\bar{e}\gamma_\mu\gamma^5 e\bar{\mu}\gamma^\mu\gamma^5\mu. \tag{2.55}$$

These terms result in an additional tree-level process which is shown in Figure 2.4. Application of the Feynman rules produces matrix elements which can all be simplified to the form:

$$\mathcal{M}_{ij} = \frac{g^2\eta}{\Lambda^2}\bar{v}(p_2)\Gamma^\mu_{ij}u(p_1)\bar{u}(p_3)\Gamma_{\mu ij}v(p_4) \tag{2.56}$$

where Γ^μ_{ij} is a matrix containing γ^μ and either the projection operators P_L or P_R, or γ^5. The projection operators are defined as

$$P_{R,L} = \frac{1}{2}(1 \pm \gamma^5), \tag{2.57}$$

and satisfy the identities

$$P_{L,R}\gamma^{\mu} = \gamma^{\mu}P_{R,L}, \tag{2.58}$$

and

$$P_{L,R}^2 = P_{L,R}. \tag{2.59}$$

Once the relevant simplifications have been made it is possible to compute the contributions to the cross section from the addition of these various terms. The three contributions from each model are are $|\mathcal{M}_{ij}|^2$ as well as the interference terms

$$\langle \mathcal{M}_{ij,\gamma} \rangle = \langle \mathcal{M}_{ij}\mathcal{M}_{\gamma}^{*} \rangle + \langle \mathcal{M}_{ij}^{*}\mathcal{M}_{\gamma} \rangle \tag{2.60}$$

$$\langle \mathcal{M}_{ij,Z} \rangle = \langle \mathcal{M}_{ij}\mathcal{M}_{Z}^{*} \rangle + \langle \mathcal{M}_{ij}^{*}\mathcal{M}_{Z} \rangle \tag{2.61}$$

These are then converted into differential cross sections and integrated over the relevant boundary conditions, just as was done for the contributions from the N^0 process. The fit was done for each model using the parameter

$$\epsilon_{4f} = \frac{1}{\Lambda^2}, \tag{2.62}$$

which we allow to take on positive and negative values in analogy with the fits for the N^0 parameters. We accompany the central value with a 1σ range of error, as well as the 95% confidence limits on Λ for each of the cases $\eta = \pm 1$. For details on the derivation of these values, see Section 2.5. The results of these fits for muons are given in Table 2.4.

This process was then repeated for the same interaction but with tauons as the resulting pair produced. These results are given in Table 2.5. The central values from these analyses were then all combined for each model by using a weighted mean, and these results are accompanied in Table 2.6 with the most stringent of the limits for $\Lambda^{\pm}$ and also the limits given by LEP [16] to show the general agreement between the results. It is worth noting that it is physically meaningless to combine central values of different signs (as these correspond to different models) so when they are averaged, the central values are taken to have the same sign (negative, by convention). The results shown in Tables 2.4 and 2.5 are provided to illustrate the range of constraints coming from different processes. It is in Table 2.6 where we compare our combined results to those found in Table 13 of [16], and

Model	ϵ_{4f} from σ	Λ^+ from σ	Λ^- from σ	ϵ_{4f} from A_{FB}	Λ^+ from A_{FB}	Λ^- from A_{FB}
VV	$-0.0023^{+0.0016}_{-0.0016}$	22.8 TeV	14.2 TeV	$-0.0035^{+0.0061}_{-0.0055}$	9.5 TeV	8.9 TeV
AA	$-0.0049^{+0.0036}_{-0.0036}$	15.6 TeV	9.4 TeV	$0.0016^{+0.0029}_{-0.0028}$	12.0 TeV	15.0 TeV
LL	$-0.0058^{+0.0041}_{-0.0041}$	14.2 TeV	8.8 TeV	$0.0152^{+0.0188}_{-0.0234}$	4.2 TeV	6.0 TeV
RR	$-0.0067^{+0.0047}_{-0.0047}$	13.3 TeV	8.2 TeV	$0.0132^{+0.0258}_{-0.0410}$	3.9 TeV	5.6 TeV
LR	$-0.0187^{+0.0131}_{-0.0154}$	8.7 TeV	0.9 TeV	$-0.0045^{+0.0077}_{-0.0076}$	8.9 TeV	7.5 TeV
RL	$-0.0187^{+0.0131}_{-0.0154}$	8.7 TeV	0.9 TeV	$-0.0045^{+0.0077}_{-0.0076}$	8.9 TeV	7.5 TeV

Table 2.4: Central values for ϵ_{4f}, and 95% confidence limits on Λ as obtained by our analysis for different four-fermion models for muon production. Here, ϵ in units of TeV^{-2} and the values were obtained from fits to the cross section, σ, and the forward-backward asymmetry, A_{FB}. Λ^+ is the 95% confidence limit obtained for $\eta = +1$, and Λ^- is the 95% confidence limit obtained for $\eta = -1$.

Model	ϵ_{4f} from σ	Λ^+ from σ	Λ^- from σ	ϵ_{4f} from A_{FB}	Λ^+ from A_{FB}	Λ^- from A_{FB}
VV	$-0.0014^{+0.0021}_{-0.0021}$	17.6 TeV	13.8 TeV	$-0.0094^{+0.0072}_{-0.0064}$	9.2 TeV	7.2 TeV
AA	$-0.0030^{+0.0045}_{-0.0048}$	12.1 TeV	9.1 TeV	$0.0048^{+0.0038}_{-0.0038}$	9.3 TeV	14.7 TeV
LL	$-0.0036^{+0.0054}_{-0.0054}$	11.0 TeV	8.6 TeV	$0.0362^{+0.0350}_{-0.0292}$	3.0 TeV	6.0 TeV
RR	$-0.0042^{+0.0062}_{-0.0063}$	10.3 TeV	8.0 TeV	$0.0416^{+0.0400}_{-0.0335}$	2.9 TeV	5.5 TeV
LR	$-0.0113^{+0.0160}_{-0.0191}$	6.9 TeV	1.0 TeV	$-0.0127^{+0.0099}_{-0.0097}$	8.7 TeV	5.9 TeV
RL	$-0.0113^{+0.0160}_{-0.0191}$	6.9 TeV	1.0 TeV	$-0.0127^{+0.0099}_{-0.0097}$	8.7 TeV	5.9 TeV

Table 2.5: Central values for ϵ_{4f}, and 95% confidence limits on Λ as obtained by our analysis for different four-fermion models for tauon production. Here, ϵ in units of TeV^{-2} and the values were obtained from fits to the cross section, σ, and the forward-backward asymmetry, A_{FB}. Λ^+ is the 95% confidence limit obtained for $\eta = +1$, and Λ^- is the 95% confidence limit obtained for $\eta = -1$.

Model	$\bar{\epsilon} \pm \delta\bar{\epsilon}$	Λ^+	Λ^-	$\epsilon \pm \delta\epsilon$ (LEP)	Λ^+ (LEP)	Λ^- (LEP)
VV	-0.0023 ± 0.0012	22.8 TeV	14.2 TeV	$-0.0016^{+0.0013}_{-0.0014}$	21.7 TeV	16.0 TeV
AA	-0.0033 ± 0.0018	16.2 TeV	12.1 TeV	$-0.0013^{+0.0017}_{-0.0017}$	17.2 TeV	15.1 TeV
LL	-0.0055 ± 0.0032	14.2 TeV	8.6 TeV	$-0.0044^{+0.0035}_{-0.0035}$	13.3 TeV	9.8 TeV
RR	-0.0062 ± 0.0037	13.3 TeV	8.2 TeV	$-0.0049^{+0.0039}_{-0.0039}$	12.7 TeV	9.3 TeV
LR	-0.0094 ± 0.0053	8.7 TeV	10.0 TeV	$-0.0036^{+0.0052}_{-0.0054}$	10.2 TeV	8.6 TeV
RL	-0.0094 ± 0.0053	8.7 TeV	10.0 TeV	$-0.0036^{+0.0052}_{-0.0054}$	10.2 TeV	8.6 TeV

Table 2.6: The averaged central values for ϵ_{4f} along with the most stringent 95% confidence limits on Λ for $\eta = \pm 1$ as obtained by our analysis are given. Values for $\bar{\epsilon}$ are given in TeV^{-2}. These are accompanied by the quoted central values, and 95% confidence limits for $\eta = \pm 1$ as obtained from Table 13 in [16].

where we clearly see the agreement with their results.

The agreement between the results from our fits and the LEP results indicate that the use of this method in obtaining limits on the N^0 signature is justified.

2.A Appendix: Feynman Rules and Trace Technology

When we are looking at scattering events in perturbative quantum field theory, it will often suffice to only consider first order expansions of the path integral. These terms, when represented by Feynman diagrams, are referred to as "Tree Level" processes. The structure of the corresponding matrix elements can be derived from the path integral and translated into a set of rules, called Feynman Rules. Here we will list the Feynman rules relevant to our processes, and we unapologetically omit the rules which apply to particles and processes not referenced in this work (See [4], [22]).

1. Incoming fermions [antifermions] receive a factor of $u(p)$ $[\bar{v}(p)]$, where p is the four momentum of the fermion, and we have suppressed the dependence of the spinor on the fermion's spin.

2. Outgoing fermions [antifermions] receive a factor of $\bar{u}(p)$ $[v(p)]$.

3. There are a few different vertices that are encountered:

   - Fermion-Photon Vertex:

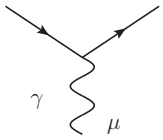

$$= \quad -ie\gamma^{\mu} \tag{2.63}$$

   - Fermion-Z Vertex:

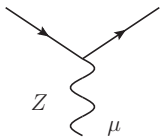

$$= \quad \frac{-ie}{2c_W^2 s_W^2}\gamma^{\mu}(C_v - C_a\gamma^5) \tag{2.64}$$

   - Fermion-N^0 Vertex:

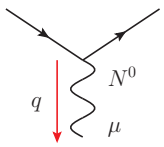

$$= \quad \frac{ig\eta}{\Lambda}q_{\nu}\sigma^{\mu\nu} \tag{2.65}$$

4. Intermediate bosons receive a propagator and there are a few of these as well:

- Photon Propagator:

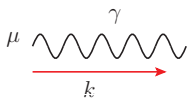

$$= \frac{-ig_{\mu\nu}}{k^2} \tag{2.66}$$

- Z Propagator:

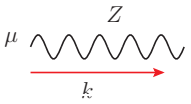

$$= \frac{-i}{k^2 - m_Z^2 + im_Z\Gamma_Z}(g_{\mu\nu} - \frac{k_\mu k_\nu}{m_Z^2}) \tag{2.67}$$

- N^0 Propagator:

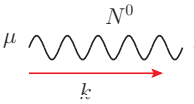

$$= \frac{-i}{k^2 - m_N^2 + im_N\Gamma_N}(g_{\mu\nu} - \frac{k_\mu k_\nu}{m_N^2}) \tag{2.68}$$

5. 4-Momentum is conserved at each vertex, corresponding to a Dirac-delta function:

$$(2\pi)^4\delta^{(4)}(p_i) \tag{2.69}$$

6. All internal momenta k_i are integrated over:

$$\prod_i \int \frac{d^4k_i}{(2\pi)^4} \tag{2.70}$$

7. Finally, an overall factor of i is dropped.

Once the Feynman rules have been applied, and the matrix elements obtained, there are still several steps which must be taken in order to obtain the differential cross section or any other measurable quantity. Rather than outlining these steps in complete generality, we will opt to use an example calculation to highlight the relevant tricks and theorems used in the derivation of a measurable quantity such as the cross section. Let's consider the interference of the the N^0 process with the photonic process. Referring to equations 2.2 and 2.11, we have

$$M_N M_\gamma^* = \frac{C_N e^2}{k^2}(q_\alpha q_\rho g_{\mu\nu})\left(g_{\delta\lambda} - \frac{q_\delta q_\lambda}{m_N^2}\right) \tag{2.71}$$
$$\times \bar{u}(p_1)\gamma^\mu v(p_2)\bar{v}(p_2)\sigma^{\delta\alpha}v(p_4)\bar{v}(p_4)\gamma^\nu u(p_3)\bar{u}(p_3)\sigma^{\rho\beta}u(p_1)$$

What we really wish to construct is the spin-averaged amplitude, in which we average over the spins of the incoming particles and sum over the spin of the outgoing particles. Though we have suppressed the notation, each spinor also has a spin, s_i, and our interference term becomes

$$\langle M_N M_\gamma^* \rangle = \frac{1}{4} \sum_{s_1,s_2} \sum_{s_3,s_4} \frac{C_N e^2}{k^2} (q_\alpha q_\rho g_{\mu\nu}) \left(g_{\delta\lambda} - \frac{q_\delta q_\lambda}{m_N^2} \right) \tag{2.72}$$
$$\times \bar{u}(p_1)\gamma^\mu v(p_2)\bar{v}(p_2)\sigma^{\delta\alpha} v(p_4)\bar{v}(p_4)\gamma^\nu u(p_3)\bar{u}(p_3)\sigma^{\lambda\rho} u(p_1)$$

At this point, we can employ the completeness relations of the spinors to simplify this expression. The completeness relations take the form

$$\sum_{s_1} u(p_1, s_1)\bar{u}(p_1, s_1) = (\not{p}_1 + m) \tag{2.73}$$
$$\sum_{s_1} v(p_1, s_1)\bar{v}(p_1, s_1) = (\not{p}_1 - m)$$

.

We will also drop all the prefactors for a moment, and write out just the spinor component of the amplitude with explicit spinor indices $\{i, j, k...\}$. Then,

$$\begin{aligned}
\langle M_N M_\gamma^* \rangle &\propto \sum_{s_1,s_2} \sum_{s_3,s_4} \bar{u}_i(p_1)(\gamma^\mu)_{ij} v_j(p_2)\bar{v}_k(p_2)(\sigma^{\delta\alpha})_{kl} v_l(p_4)\bar{v}_m(p_4)(\gamma^\nu)_{mn} u_n(p_3)\bar{u}_o(p_3)(\sigma^{\lambda\rho})_{op} u_p(p_1) \\
&= \sum_{s_1} \bar{u}_i(p_1)(\gamma^\mu)_{ij}(\not{p}_2 - m_e)_{jk}(\sigma^{\delta\alpha})_{kl}(\not{p}_4 - m_\mu)_{lm}(\gamma^\nu)_{mn}(\not{p}_3 + m_\mu)_{no}(\sigma^{\lambda\rho})_{op} u_p(p_1) \\
&= (\not{p}_1 + m_e)_{pi}(\gamma^\mu)_{ij}(\not{p}_2 - m_e)_{jk}(\sigma^{\delta\alpha})_{kl}(\not{p}_4 - m_\mu)_{lm}(\gamma^\nu)_{mn}(\not{p}_3 + m_\mu)_{no}(\sigma^{\lambda\rho})_{op} \\
&= Tr[(\not{p}_1 + m_e)\gamma^\mu(\not{p}_2 - m_e)\sigma^{\delta\alpha}(\not{p}_4 - m_\mu)\gamma^\nu(\not{p}_3 + m_\mu)\sigma^{\lambda\rho}]
\end{aligned} \tag{2.74}$$

This last step, where we have used the fact that all indices are summed over, which is the definition of the Trace over a given matrix, greatly simplifies the amplitude and is sometimes referred to as Casimir's Trick [12]. All that is required now are some strategies for evaluating this trace, and traces like this which arise in other similar calculations. For this, we outline a few simple rules which can be followed.

- The trace of any odd number of γ matrices is zero.
- The trace of two gamma matrices is

$$Tr[\gamma^\mu \gamma^\nu] = 4g^{\mu\nu} \tag{2.75}$$

- The trace of any even number, n, of γ matrices can be turned into a sum of traces containing n-2 γ matrices by using the fundamental anticommutation relation of the γ matrices:

$$\{\gamma^\mu, \gamma^\nu\} = 2g^{\mu\nu} \tag{2.76}$$

.

The number of Lorentz indices will be conserved by multiplying by the appropriate number of metrics. For example,

$$\begin{aligned}
Tr[\gamma^\alpha\gamma^\beta\gamma^\mu\gamma^\nu] &= Tr[(2g^{\alpha\beta} - \gamma^\beta\gamma^\alpha)\gamma^\mu\gamma^\nu] \\
&= 2g^{\alpha\beta}Tr[\gamma^\mu\gamma^\nu] - Tr[\gamma^\beta(2g^{\alpha\mu} - \gamma^\mu\gamma^\alpha)\gamma^\nu] \\
&= 2g^{\alpha\beta}Tr[\gamma^\mu\gamma^\nu] - 2g^{\alpha\mu}Tr[\gamma^\beta\gamma^\nu] + Tr[\gamma^\beta\gamma^\mu(2g^{\alpha\nu} - \gamma^\nu\gamma^\alpha)] \\
&= 2g^{\alpha\beta}Tr[\gamma^\mu\gamma^\nu] - 2g^{\alpha\mu}Tr[\gamma^\beta\gamma^\nu] + 2g^{\alpha\nu}Tr[\gamma^\beta\gamma^\mu] - Tr[\gamma^\beta\gamma^\mu\gamma^\nu\gamma^\alpha] \\
\rightarrow Tr[\gamma^\alpha\gamma^\beta\gamma^\mu\gamma^\nu] &= g^{\alpha\beta}Tr[\gamma^\mu\gamma^\nu] - g^{\alpha\mu}Tr[\gamma^\beta\gamma^\nu] + g^{\alpha\nu}Tr[\gamma^\beta\gamma^\mu] \\
&= 4(g^{\alpha\beta}g^{\mu\nu} - g^{\alpha\mu}g^{\beta\nu} + g^{\alpha\nu}g^{\beta\mu})
\end{aligned} \tag{2.77}$$

where, in going from the third last step to the second last step, we have used the cyclicity property of traces

$$Tr[ABC] = Tr[CAB] = Tr[BCA] \tag{2.78}$$

to obtain

$$Tr[\gamma^\beta\gamma^\mu\gamma^\nu\gamma^\alpha] = Tr[\gamma^\alpha\gamma^\beta\gamma^\mu\gamma^\nu] \tag{2.79}$$

This procedure can, in principle, be done for a trace of any length, however as the number of γ matrices increases, the number of terms increases very rapidly. Looking back at equation 2.74, it is clear that our longest trace will contain ten gamma matrices. For this reason, a Mathematica program was devised and used in the evaluation of these matrix elements.

- Many of the traces (eg. ones involving the Z boson, or the chiral four-fermion terms) will involve γ^5, and while there are several tricks for handling this among small numbers of γ matrices, the code used employs the definition

$$\gamma^5 = \frac{-i}{4!}\epsilon^{\alpha\beta\mu\nu}\gamma_\alpha\gamma_\beta\gamma_\mu\gamma_\nu \tag{2.80}$$

such that even traces involving, for example, ten γ's and a γ^5 may be easily evaluated. The fully antisymmetric pseudotensor $\epsilon^{\alpha\beta\mu\nu}$ is defined as

$$\epsilon^{\alpha\beta\mu\nu} = \begin{cases} 1 & \text{for even permutations of } \{\alpha,\beta,\mu,\nu\} \\ -1 & \text{for odd permutations of } \{\alpha,\beta,\mu,\nu\} \\ 0 & \text{otherwise} \end{cases} \tag{2.81}$$

In practice, we are occasionally faced with products of ϵ tensors and these can be dealt with using the following determinant formula [15]:

$$\epsilon_{\mu_1\mu_2\mu_3\mu_4}\epsilon_{\nu_1\nu_2\nu_3\nu_4} = \begin{vmatrix} \delta_{\mu_1\nu_1} & \delta_{\mu_1\nu_2} & \delta_{\mu_1\nu_3} & \delta_{\mu_1\nu_4} \\ \delta_{\mu_2\nu_1} & \delta_{\mu_2\nu_2} & \delta_{\mu_2\nu_3} & \delta_{\mu_2\nu_4} \\ \delta_{\mu_3\nu_1} & \delta_{\mu_3\nu_2} & \delta_{\mu_3\nu_3} & \delta_{\mu_3\nu_4} \\ \delta_{\mu_4\nu_1} & \delta_{\mu_4\nu_2} & \delta_{\mu_4\nu_3} & \delta_{\mu_4\nu_4} \end{vmatrix} \tag{2.82}$$

which, of course, simplifies drastically when any of the μ_i's are equal to the ν_j's.

2.B Appendix: Mandelstam Variables and Kinematics

Once evaluated, the traces found in simplifying the products of matrix elements will be given in terms of momenta contractions, and potentially contractions of momenta with the ϵ tensor. It is conventional to substitute these products for the so-called Mandelstam variables which are defined as

$$\begin{aligned} s &= (p_1+p_2)^2 \\ t &= (p_1-p_3)^2 \\ u &= (p_1-p_4)^2. \end{aligned} \tag{2.83}$$

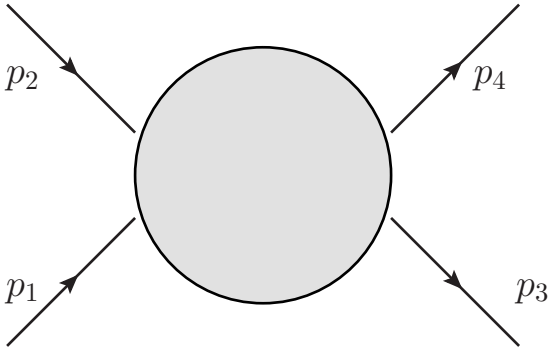

Figure 2.5: Kinematic conventions for a general two-body to two-body Feynman diagram. Here the dark circle is indicative of arbitrary processes occurring between the initial and final states.

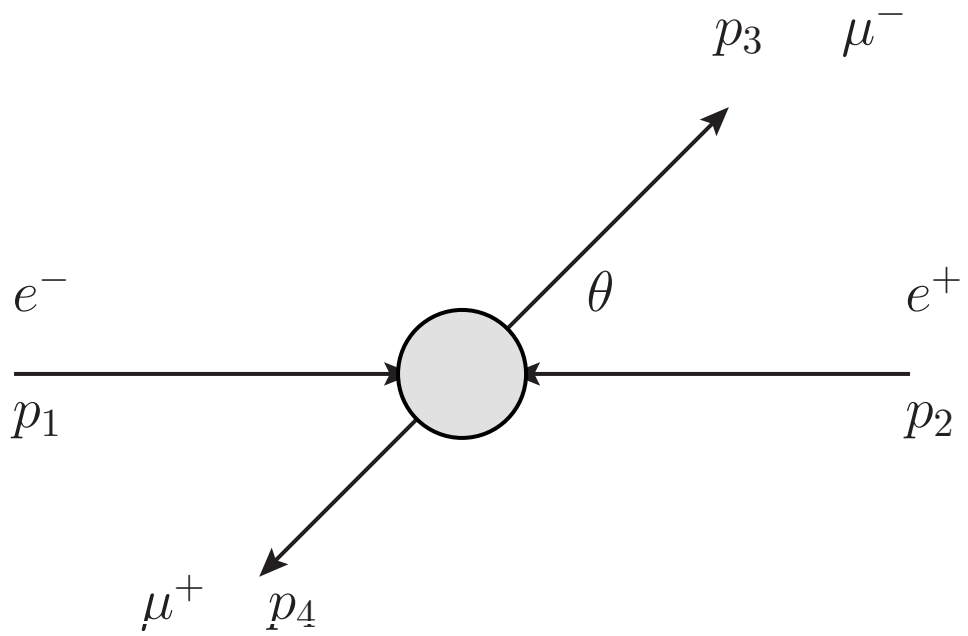

Figure 2.6: Kinematic conventions in the center of mass frame, with the particle types specific to $e^+e^- \to \mu^+\mu^-$ scattering indicated. As mentioned in Section 2.1, θ is defined as the angle between the trajectories of p_1 and p_3.

where $\{p_1, p_2, p_3, p_4, \}$ are defined in Figures 2.5 and 2.6. These are useful because they are Lorentz invariant and are thus a compact way to discuss the results of a calculation without referring to a particular experimental set up, or choice of reference frame. These variables also satisfy a very useful relation

$$s + t + u = \sum_i m_i^2 \tag{2.84}$$

where m_i is the mass of particle i, and the sum over i is over all of the particles involved. These variables can then be expressed in terms of kinematic variables, depending on what is needed. We have given all of our differential cross sections in terms of the center-of-mass frame, so here we present the conversion used from Mandelstam variables to kinematic variables for the particular process $e^+e^- \to \mu^-\mu^+$.

$$\begin{aligned} s &= 4E^2 \\ t &= -2E^2 + m_e^2 + m_\mu^2 + \sqrt{(E^2 - m_e^2)(E^2 - m_\mu^2)}\cos\theta \\ u &= -2E^2 + m_e^2 + m_\mu^2 - \sqrt{(E^2 - m_e^2)(E^2 - m_\mu^2)}\cos\theta \end{aligned} \tag{2.85}$$

2.C Appendix: A_{FB} for the N^0

Here we give the exact expressions obtained for the calculation of the forward-backward asymmetry for the N^0 contributions. The odd numerical factors arise from the integration limits of 0.94 and -0.94 as opposed to 1 and -1. For the heavy N^0, the parameter ϵ has been scaled as

$$\epsilon = \frac{10^{-14}}{\Lambda^2 m_N^2} \tag{2.86}$$

in order to prevent Mathematica from dropping important terms with apparently small coefficients. The exact expression we find is

$$\begin{aligned} A_{FB}^h = \quad & \tfrac{1}{F_h(E)} \left(E^2 \left(C_A^2 \left(1.77 \times 10^{14} \alpha C_V^2 E^2 + c_W^2 s_W^2 \left(16.11E^6\epsilon - 4.03E^4 m_Z^2 \epsilon + 3.53 \times 10^{14}\alpha E^2\right.\right.\right.\right. \\ & - \left.\left.\left.\left. 8.84 \times 10^{13} \alpha m_Z^2\right)\right) + c_W^2 E^2 s_W^2 \epsilon \left(C_V^2 \left(4.03E^2 m_Z^2 - 16.11E^4\right) + \right.\right. \right. \\ & \left.\left.\left. c_W^2 s_W^2 \left(-64.44E^4 + 32.22E^2 m_Z^2 - 4.03 m_Z^4 - 4.03\Gamma_Z^2 m_Z^2\right)\right)\right)\right) \end{aligned} \tag{2.87}$$

where the denominator function $F_h(E)$ is found to be

$$F_h(E) = \left(6.08 \times 10^{13} \alpha C_A^4 E^4 + C_A^2 \left(1.22 \times 10^{14} \alpha C_V^2 E^4 + c_W^2 E^6 s_W^2 \epsilon \left(6.19 m_Z^2 - 24.77 E^2\right)\right)\right.$$
$$+6.08 \times 10^{13} \alpha C_V^4 E^4 + C_V^2 c_W^2 E^2 s_W^2 \left(24.77 E^6 \epsilon - 6.19 E^4 m_Z^2 \epsilon + 4.87 \times 10^{14} \alpha E^2 -\right.$$
$$\left.1.22 \times 10^{14} \alpha m_Z^2\right) + 99.10 c_W^4 E^8 s_W^4 \epsilon - 49.55 c_W^4 E^6 m_Z^2 s_W^4 \epsilon + 6.19 c_W^4 E^4 m_Z^4 s_W^4 \epsilon +$$
$$6.19 c_W^4 \Gamma_Z^2 E^4 m_Z^2 s_W^4 \epsilon + 9.73 \times 10^{14} \alpha c_W^4 E^4 s_W^4 - 4.87 \times 10^{14} \alpha c_W^4 E^2 m_Z^2 s_W^4 + 6.08 \times 10^{13} \alpha c_W^4 m_Z^4 s_W^4$$
$$\left.+6.08 \times 10^{13} \alpha c_W^4 \Gamma_Z^2 m_Z^2 s_W^4\right). \tag{2.88}$$

For the light N^0, ϵ has different dimensions and thus is scaled differently to

$$\epsilon = \frac{10^{-8}}{\Lambda^2} \tag{2.89}$$

and the resulting expression for the forward-backward asymmetry is

$$A_{FB}^l = \tfrac{1}{F_l(E)} \left(E^2 \left(C_A^2 \left(7.07 \alpha C_V^2 E^2 + c_W^2 s_W^2 \left(1.41 \times 10^{-7} E^4 \epsilon + E^2 \left(14.14 \alpha - 3.53 \times 10^{-8} m_Z^2 \epsilon\right)\right.\right.\right.\right.$$
$$\left.\left.-3.53 \alpha m_Z^2\right)\right) + c_W^2 s_W^2 \epsilon \left(C_V^2 \left(3.53 \times 10^{-8} E^2 m_Z^2 - 1.41 \times 10^{-7} E^4\right) + c_W^2 s_W^2 \left(-5.66 \times 10^{-7} E^4\right.\right.$$
$$\left.\left.\left.\left.+2.83 \times 10^{-7} E^2 m_Z^2 - 3.53 \times 10^{-8} m_Z^4 - 3.53 \times 10^{-8} \Gamma_Z^2 m_Z^2\right)\right)\right)\right) \tag{2.90}$$

with $F_l(E)$ found to be

$$F_l(E) = \left(2.43 \alpha C_A^4 E^4 + C_A^2 E^4 \left(4.87 \alpha C_V^2 + c_W^2 s_W^2 \epsilon \left(1.02 \times 10^{-7} m_Z^2 - 4.07 \times 10^{-7} E^2\right)\right)\right.$$
$$+2.43 \alpha C_V^4 E^4 + C_V^2 c_W^2 E^2 s_W^2 \left(4.07 \times 10^{-7} E^4 \epsilon + E^2 \left(19.47 \alpha - 1.02 \times 10^{-7} m_Z^2 \epsilon\right)\right.$$
$$\left.-4.87 \alpha m_Z^2\right) + 1.63 \times 10^{-6} c_W^4 E^6 s_W^4 \epsilon - 8.14 \times 10^{-7} c_W^4 E^4 m_Z^2 s_W^4 \epsilon + 38.94 \alpha c_W^4 E^4 s_W^4$$
$$+1.02 \times 10^{-7} c_W^4 E^2 m_Z^4 s_W^4 \epsilon - 19.47 \alpha c_W^4 E^2 m_Z^2 s_W^4 + 1.02 \times 10^{-7} c_W^4 \Gamma_Z^2 E^2 m_Z^2 s_W^4 \epsilon +$$
$$\left.2.43 \alpha c_W^4 m z^4 s_W^4 + 2.43 \alpha c_W^4 \Gamma_Z^2 m_Z^2 s_W^4\right) \tag{2.91}$$

The χ^2 functions constructed from these expressions are highly non-linear, and so in the interest of reducing the task set to Mathematica, the χ^2 expressions were expanded in powers of ϵ. To ensure that we did not lose too much detail, we kept ten powers of ϵ in the analysis. The values resulting from minimizing these functions could then be divided by 100 in both cases to give our parameters in TeV for the light case and TeV^2 for the heavy case.

Chapter 3

Constraints from Muonium - Antimuonium Oscillations

Muonium is a neutral hydrogen-like bound state which occurs when an electron becomes trapped by the coulomb potential of an antimuon [27]. Antimuonium then, is the bound state that forms when a positron gets trapped in the coulomb potential of a muon. Once the electron is captured by the muon (or vice versa), and a bound state is formed, the system can be safely treated in a non relativistic regime and the behaviour of this electron is exactly the same as the electron in a hydrogen atom. To see that we may safely treat this system non-relativistically, we need only take the root-mean-square of the velocity of the ground state electron relative to the muon nucleus. In the standard $\{|n,l,m\rangle\}$ basis of the hydrogen atom, we can calculate

$$\begin{aligned} \langle v^2 \rangle &= \langle 100| \frac{p^2}{m^2} |100\rangle \\ &= -\frac{1}{m_e^2} \int d^3r \; \psi^*_{100}(r) \nabla^2 \psi_{100}(r) \\ &= \alpha^2 \end{aligned} \tag{3.1}$$

where the ground state wavefunction is given by

$$\psi_{100}(r) = \frac{1}{\sqrt{\pi a^3}} e^{-\frac{r}{a}} \tag{3.2}$$

which tells us that

$$\sqrt{\langle v^2 \rangle} = \alpha, \qquad \text{or, restoring the speed of light,} \quad \approx \frac{c}{137} \tag{3.3}$$

which is sufficiently slow that relativistic corrections may be safely neglected for our purposes. Once formed, this bound state will only continue to exist until the muon (or antimuon) decays via the weak interaction. In the SM, there is no mechanism which would allow for muonium to transform into antimuonium, as this would be a violation of both electron and muon numbers. Some extensions of the SM, including the one being studied here, include mechanisms for these muonium-antimuonium oscillations to occur. Experimentally, the constraints on muonium decaying like antimuonium are fairly stringent, which allows theorists to put bounds on their models for physics beyond the SM.

The calculation will go as follows. The first order matrix elements, $\mathcal{M}$, will be obtained from the mechanism in question which converts muonium, M, into antimuonium, $\bar{M}$, and expanded in the non-relativistic limit. To clarify, the Scattering Matrix, S, is unitary and is defined as [22]

$$S = I + iT \tag{3.4}$$

where I is the identity matrix (no scattering at all) and T, called the *T Matrix*, which embodies all of the details of the scattering process. The T matrix is then related to the full matrix elements by the relation

$$\langle p_1 p_2 | iT | k_1 k_2 \rangle = (2\pi)^4 \delta^{(4)}(k_1 + k_2 - p_1 + p_2) i\mathcal{M}, \tag{3.5}$$

of which we are interested in calculating the tree-level, or first order, expression of. Following [22] in our methodology, these expanded matrix elements can be compared with Born approximation to the non-relativistic scattering amplitude and written in terms of a potential $V(r)$. To do this, we use

$$\langle p' | iT | p \rangle = -i\tilde{V}(\mathbf{q})(2\pi)\delta(E_{\mathbf{p}'} - E_{\mathbf{p}}), \qquad (\mathbf{q} = \mathbf{p}' - \mathbf{p}), \tag{3.6}$$

and the potential $V(r)$ can be obtained from $\tilde{V}(\mathbf{q})$ by way of an inverse Fourier Transform:

$$V(r) = \int \frac{d^3q}{(2\pi)^3} \tilde{V}(\mathbf{q}) e^{iq \cdot r} \tag{3.7}$$

We will treat this potential as a perturbation to a generalized Hamilton H_0 and use first order

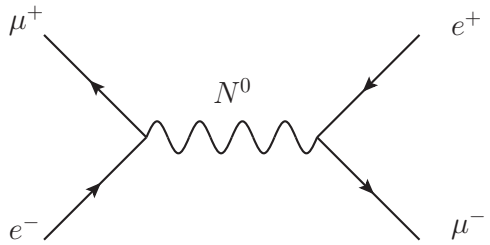

Figure 3.1: The s-channel diagram contributing to muonium-antimuonium oscillation via the N^0.

perturbation theory to calculate the expectation value for these interactions on the ground state of muonium, averaging over the singlet and triplet spin configurations. That is, we will calculate

$$\begin{aligned} \langle V(r) \rangle &= \langle \bar{M} | \delta V | M \rangle \\ &= \int d^3r |\psi(r)|^2 \delta V(r) \end{aligned} \tag{3.8}$$

where $\psi(r)$ is the unperturbed wavefunction of the muonium electron. From there, we will obtain the probability that muonium decays as anti-muonium as a function of $\langle V(r) \rangle$, and compare this to the experimental bounds. This comparison will allow us to set bounds on the parameters of the model in question.

3.1 N^0: The Heavy Case

For the dipole transition mediated by the N^0, there are two Feynman diagrams that contribute to the conversion of muonium into antimuonium, an s-channel diagram and a t-channel diagram. See Figures 3.1 and 3.2. We will label the matrix elements associated with the two diagrams as $\mathcal{M}_s$ for the s-channel and $\mathcal{M}_t$ for the t-channel, with the total matrix element being given by

$$\mathcal{M} = \mathcal{M}_s + \mathcal{M}_t \tag{3.9}$$

In keeping with our conventions from the scattering analysis, we will use the momenta

$$\begin{aligned} k &= \sqrt{s} = p_1 + p_2 \\ q &= \sqrt{t} = p_1 - p_3 \end{aligned} \tag{3.10}$$

and we label the momenta of the fermions as p_1 for the antimuon, p_2 for the electron, p_3 for the

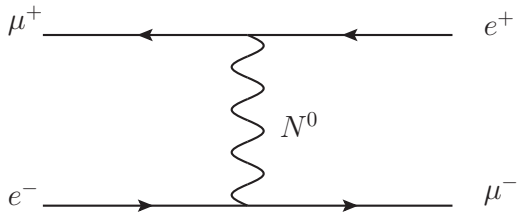

Figure 3.2: The t-channel diagram contributing to muonium-antimuonium oscillation via the N^0.

positron, and p_4 for the muon. It is worth noting that while the t-channel choice is inconsistent with the conventions outlined in Appendix 2.B, this is of no consequence, since we will drop all orders of momenta in our analysis.

In the heavy N^0 scenario, we can simplify our matrix elements to

$$\begin{aligned}\mathcal{M}_s &= -\frac{g}{(\Lambda m_N)^2} k_\nu k_\beta g_{\mu\alpha} \bar{u}(p_4)\sigma^{\mu\nu} v(p_3)\bar{v}(p_1)\sigma^{\alpha\beta} u(p_2) \\ \mathcal{M}_t &= -\frac{g}{(\Lambda m_N)^2} q_\nu q_\beta g_{\mu\alpha} \bar{u}(p_4)\sigma^{\mu\nu} u(p_2)\bar{v}(p_1)\sigma^{\alpha\beta} v(p_3).\end{aligned} \tag{3.11}$$

The task now will be to expand these terms in the non-relativistic limit. For details on this process and a sample calculation, refer to Appendix 3.A. Here we will state the results in terms of the 2-spinors ξ_l for particles and η_l for antiparticles ($l = e, \mu$). The relationship between these spinors and the relativistic spinors $u(p)$ and $v(p)$ is given in Appendix 3.A, but we will note that these spinors are normalized such that $\xi^\dagger\xi = \eta^\dagger\eta = 1$ and that

$$\sum \xi\xi^\dagger = \sum \eta\eta^\dagger = I \tag{3.12}$$

.

where I is the two-by-two identity matrix. The expanded matrix elements are

$$\begin{aligned}\mathcal{M}_s &= \frac{g^2}{(\Lambda m_N)^2}(m_e + m_\mu)^2 \bar{\eta}_\mu \boldsymbol{\sigma} \xi_e \cdot \bar{\xi}_\mu \boldsymbol{\sigma} \eta_e \\ \mathcal{M}_t &= 0,\end{aligned} \tag{3.13}$$

where here, $\boldsymbol{\sigma}$ is defined in Equation 1.4. Our combined amplitude is

$$\mathcal{M} = \mathcal{M}_s = \frac{g^2}{(\Lambda m_N)^2}(m_e + m_\mu)^2 \bar{\eta}_\mu \boldsymbol{\sigma} \xi_e \cdot \bar{\xi}_\mu \boldsymbol{\sigma} \eta_e \tag{3.14}$$

At this point we will drop the mass of the electron for the simplified result,

$$\mathcal{M} = \frac{g^2 m_\mu^2}{(\Lambda m_N)^2} \bar{\eta}_\mu \boldsymbol{\sigma} \xi_e \cdot \bar{\xi}_\mu \boldsymbol{\sigma} \eta_e \tag{3.15}$$

We can turn this amplitude into a a potential $V(r)$ by taking the fourier transform. Because there is no dependence on the momenta, this is trivial:

$$\begin{aligned} V(r) &= \int \frac{d^3k}{(2\pi)^3} e^{ik\cdot x} \mathcal{M} \\ &= \frac{g^2 m_\mu^2}{(\Lambda m_N)^2} \delta^3(r) \bar{\eta}_\mu \boldsymbol{\sigma} \xi_e \cdot \bar{\xi}_\mu \boldsymbol{\sigma} \eta_e \end{aligned} \tag{3.16}$$

The delta function form of this potential is no accident: by assuming a very heavy mediator we have effectively eliminated the dependence of $\mathcal{M}$ on the particle's momenta. This is equivalent to saying that we have reduced what would be a short ranged force to a contact potential. What we wish to do now is evaluate this in terms of the singlet and triplet spin configurations of the ground state. Explicitly, for the singlet transition we have

$$\frac{1}{\sqrt{2}} \frac{1}{\sqrt{2}} \left(\langle + - |_{\bar{M}} - \langle - + |_{\bar{M}} \right) V(r) \left(| - + \rangle_M - | + - \rangle_M \right) = \frac{2 g^2 m_\mu^2}{\Lambda^2 m_N^2} \delta^3(r) \tag{3.17}$$

and for the three triplet transitions, we have

$$\begin{aligned} \frac{1}{\sqrt{2}} \frac{1}{\sqrt{2}} \left(\langle + - |_{\bar{M}} + \langle - + |_{\bar{M}} \right) V(r) \left(| - + \rangle_M + | + - \rangle_M \right) &= 0, \\ \langle + + | V(r) | + + \rangle &= \frac{2 g^2 m_\mu^2}{\Lambda^2 m_N^2} \delta^3(r), \\ \langle - - | V(r) | - - \rangle &= \frac{2 g^2 m_\mu^2}{\Lambda^2 m_N^2} \delta^3(r), \end{aligned} \tag{3.18}$$

where we have chosen the basis for muonium of $|\xi_e \eta_\mu\rangle$ and for antimuonium $|\eta_e \xi_\mu\rangle$. We will now incorporate the spatial part of the unperturbed wavefunction. Since muonium is electromagnetically identical to the hydrogen atom, we may use the hydrogenic ground state wavefunction:

$$\psi(r) = \frac{1}{\sqrt{4\pi}} \frac{2}{a^{\frac{3}{2}}} e^{-\frac{r}{a}}. \tag{3.19}$$

Here, a is the Bohr radius, defined (in natural units) in terms of the electromagnetic fine structure

constant α and the mass of the electron as

$$a = \frac{1}{m_e \alpha} \tag{3.20}$$

All of the potentials we will be considering in this work will be $\delta(r)$ potentials, so we can generally compute the contribution from the spatial wavefunction:

$$\begin{aligned} |\psi(0)|^2 &= \int d^3r \; \delta^{(3)}(r)|\psi(r)|^2 \\ &= \frac{4}{a^3(4\pi)} \int (4\pi) r^2 dr \frac{\delta(r)}{4\pi r^2} e^{-\frac{2r}{a}} \\ &= \frac{1}{\pi a^3} \end{aligned} \tag{3.21}$$

Just as in relativistic scattering, where we square the matrix elements $\mathcal{M}$ and then average over the possible states of the particles, the squared average of our ground state spin configurations give

$$\begin{aligned} \langle V^2 \rangle &= \frac{3}{4} \left(\frac{2g^2 m_\mu^2}{\pi a^3 \Lambda^2 m_N^2} \right)^2 \\ &= \frac{3g^4 m_\mu^4}{\pi^2 a^6 \Lambda^4 m_N^4} \end{aligned} \tag{3.22}$$

Very generally, for a Hamiltonian of the form

$$H_0 = \begin{pmatrix} E_M & \frac{\delta}{2} \\ \frac{\delta}{2} & E_{\bar{M}} \end{pmatrix} \tag{3.23}$$

in the basis

$$\begin{pmatrix} M \\ \bar{M} \end{pmatrix} \tag{3.24}$$

the probability that muonium will decay as antimuonium is given by [9] as (See Appendix 3.B for details on this calculation)

$$P(\bar{M}) = \frac{\delta^2}{2\Gamma_\mu^2} \tag{3.25}$$

where

$$\Gamma_\mu = \frac{G_F^2 m_\mu^5}{192\pi^3} \approx 3.0 \times 10^{-19}\ \text{GeV} \tag{3.26}$$

is the muon decay width, G_F is the Fermi constant, and in this case (subbing in $g^2 = 4\pi$),

$$\begin{aligned} \frac{\delta}{2} &= \sqrt{|\langle V^2 \rangle|} \\ &= \frac{\sqrt{48} m_\mu^2}{a^3 \Lambda^2 m_N^2}. \end{aligned} \tag{3.27}$$

Taking Equation 3.25 and setting it equal to the experimental limit on $P(\bar{M})$ of 8.2×10^{-11} set by [27] gives us

$$\Lambda m_N \approx 3.0 \times 10^{-2}\ \text{GeV}^2 \tag{3.28}$$

which is much smaller than the least stringent bounds set by any of the scattering processes analyzed in Section 2.5. We note here that we have left the analysis of the Light N^0 for future work, as it may provide bounds which are more interesting than those found for the heavy N^0. In the following sections, we will compare our results with the results of two other models, the Feinberg-Weinberg Model and the Bilepton Model, to gauge the effectiveness of our methods.

3.2 The Feinberg-Weinberg Model

One of the earliest models for muonium-antimuonium conversion was examined by Feinberg and Weinberg [9]. They postulated an interaction of the form

$$H_{int} = C\bar{\mu}\gamma^\lambda(1+\gamma^5)e\bar{\mu}\gamma_\lambda(1+\gamma^5)e + H.C., \tag{3.29}$$

where e, μ are the electron and muon fields, and C is the coupling strength, which they set equal to the Fermi constant $G_F = 1.166 \times 10^{-5}\ \text{GeV}^{-2}$. This $(V+A)\times(V+A)$ interaction, as well as a $(V-A)\times(V-A)$ interaction, was later studied as the effective interaction associated with left-right

symmetric models [13] (and see Section 1.2 for details). Our matrix element of interest, $\mathcal{M}_{FW}$ will be given by

$$\mathcal{M}_{FW} = \langle e^+(p_3), \mu^-(p_4)|H_{int}|e^-(p_1), \mu^+(p_2)\rangle \tag{3.30}$$

which we can expand using Wick's Theorem to obtain

$$\begin{aligned}\mathcal{M}_{FW} &= 2C\left[\bar{v}_\mu(p_1)\gamma^\lambda(1+\gamma^5)u_e(p_2)\bar{u}_\mu(p_4)\gamma_\lambda(1+\gamma^5)v_e(p_3)\right.\\ &- \left.\bar{v}_\mu(p_1)\gamma^\lambda(1+\gamma^5)v_e(p_3)\bar{u}_\mu(p_4)\gamma_\lambda(1+\gamma^5)u_e(p_2)\right]\end{aligned} \tag{3.31}$$

When we expand this in terms of the two-spinors $\{\eta, \xi\}$, we get the resulting expression

$$\mathcal{M}_{FW} = 2C\left[\bar{\eta}_\mu\xi_e\bar{\xi}_\mu\eta_e - \bar{\eta}_\mu\eta_e\bar{\xi}_\mu\xi_e - \bar{\eta}_\mu\boldsymbol{\sigma}\xi_e\cdot\bar{\xi}_\mu\boldsymbol{\sigma}\eta_e + \bar{\eta}_\mu\boldsymbol{\sigma}\eta_e\cdot\bar{\xi}_\mu\boldsymbol{\sigma}\xi_e\right]. \tag{3.32}$$

Just as in the case of the heavy N^0, the absence of momentum dependence leaves us with a trivial conversion of matrix element to potential $V(r)$, giving

$$V(r) = 2C\delta^{(3)}(r)\left[\bar{\eta}_\mu\xi_e\bar{\xi}_\mu\eta_e - \bar{\eta}_\mu\eta_e\bar{\xi}_\mu\xi_e - \bar{\eta}_\mu\boldsymbol{\sigma}\xi_e\cdot\bar{\xi}_\mu\boldsymbol{\sigma}\eta_e + \bar{\eta}_\mu\boldsymbol{\sigma}\eta_e\cdot\bar{\xi}_\mu\boldsymbol{\sigma}\xi_e\right] \tag{3.33}$$

which we can now evaluate in the singlet and triplet states. For the singlet, we obtain

$$\frac{1}{\sqrt{2}}\frac{1}{\sqrt{2}}\left(\langle +-|_{\bar{M}} - \langle -+|_{\bar{M}}\right)V(r)\left(|-+\rangle_M - |+-\rangle_M\right) = -8C\delta^{(3)}(r) \tag{3.34}$$

and for the triplet states, we get

$$\begin{aligned}\frac{1}{\sqrt{2}}\frac{1}{\sqrt{2}}\left(\langle +-|_{\bar{M}} + \langle -+|_{\bar{M}}\right)V(r)\left(|-+\rangle_M + |+-\rangle_M\right) &= 8C\delta^{(3)}(r),\\ \langle ++|V(r)|++\rangle &= -8C\delta^{(3)}(r),\\ \langle --|V(r)|--\rangle &= -8C\delta^{(3)}(r).\end{aligned} \tag{3.35}$$

If we now include the spatial wavefunction contribution, square, and average, we get

$$\frac{\delta}{2} = \sqrt{|\langle V^2\rangle|} = \frac{8C}{\pi a^3}, \tag{3.36}$$

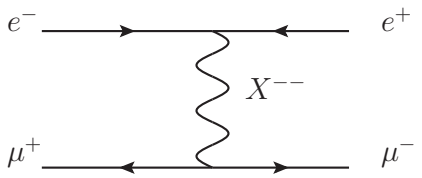

Figure 3.3: The tree level process from the double charged X^{--} bilepton contributing to muonium-antimuonium oscillation [11].

which is in agreement with [9]. Following the previous section, we have the probability for muonium-antimuonium given by

$$P(\bar{M}) = \frac{\delta^2}{2\Gamma_\mu} \approx 2.5 \times 10^{-5} \tag{3.37}$$

which is exactly the result obtained by Feinberg and Weinberg. It is worth noting that despite the agreement with [9], they report finding $\langle \bar{M}|V|M\rangle = \frac{\delta}{2}$ for all spin configurations, which is not what we find. Specifically, they find no differences between any of the singlet and triplet states, whereas we find three of the states giving a negative rather than a positive value for δ. At the present time, the source of this discrepancy is unknown, though our reproduction of the physically meaningful values suggests that it is somewhat trivial.

3.3 The Bilepton Model

Another model that has been examined for muonium-antimuonium oscillations comes from the study of 3-3-1 Models, which are explained in greater detail in Section 1.2. The Lagrangian in Equation 1.8 leads to a tree level contribution to muonium-antimuonium oscillation through Figure 3.3, and gives rise to an effective interaction Hamiltonian of the form [11]

$$H_{int} = A\bar{\mu}\gamma_\lambda(1-\gamma^5)e\bar{\mu}\gamma^\lambda(1+\gamma^5)e + H.C. \tag{3.38}$$

where

$$A = -\frac{g_{3L}^2}{8M_\chi^2} \tag{3.39}$$

and M_χ is the mass of the bilepton. We are then interested in the matrix element

$$\langle e^+(p_3), \mu^-(p_4)|H_{int}|e^-(p_1), \mu^+(p_2)\rangle \tag{3.40}$$

which we expand using Wick's theorem to obtain

$$\begin{aligned}
\langle \bar{M}|H_{int}|M\rangle &= A\left[\bar{v}_\mu(p_1)\gamma^\lambda(1+\gamma^5)u_e(p_2)\bar{u}_\mu(p_4)\gamma^\lambda(1-\gamma^5)v_e(p_3)\right. \\
&+ \bar{v}_\mu(p_1)\gamma^\lambda(1-\gamma^5)u_e(p_2)\bar{u}_\mu(p_4)\gamma^\lambda(1+\gamma^5)v_e(p_3) \\
&- \bar{v}_\mu(p_1)\gamma^\lambda(1+\gamma^5)v_e(p_3)\bar{u}_\mu(p_4)\gamma^\lambda(1-\gamma^5)u_e(p_2) \\
&- \left.\bar{v}_\mu(p_1)\gamma^\lambda(1-\gamma^5)v_e(p_2)\bar{u}_\mu(p_4)\gamma^\lambda(1+\gamma^5)u_e(p_2)\right]
\end{aligned} \tag{3.41}$$

Upon expanding these terms in the non-relativistic regime in terms of the two-spinors $\{\eta, \xi\}$, we get

$$\langle \bar{M}|H_{int}|M\rangle = 2A(\bar{\eta}_\mu\eta_e\bar{\xi}_\mu\xi_e - \bar{\eta}_\mu\xi_e\bar{\xi}_\mu\eta_e - \bar{\eta}_\mu\boldsymbol{\sigma}\xi_e\cdot\bar{\xi}_\mu\boldsymbol{\sigma}\eta_e - \bar{\eta}_\mu\boldsymbol{\sigma}\eta_e\cdot\bar{\xi}_\mu\boldsymbol{\sigma}\xi_e) \tag{3.42}$$

which we can now turn into a potential, V(r), and evaluate for the different spin configurations. The form of the potential again is a simple $\delta^{(3)}(r)$, so when we incorporate the unperturbed spatial wavefunction part it will be the same as in the previous sections. We present all these steps at once here. For the singlet, we find

$$\frac{1}{\sqrt{2}}\frac{1}{\sqrt{2}}\left(\langle +-|_{\bar{M}} - \langle -+|_{\bar{M}}\right)V(r)\left(|-+\rangle_M - |+-\rangle_M\right) = -\frac{4A}{\pi a^3}, \tag{3.43}$$

and for the triplet states we find

$$\begin{aligned}
\frac{1}{\sqrt{2}}\frac{1}{\sqrt{2}}\left(\langle +-|_{\bar{M}} + \langle -+|_{\bar{M}}\right)V(r)\left(|-+\rangle_M + |+-\rangle_M\right) &= -\frac{12A}{\pi a^3}, \\
\langle ++|V(r)|++\rangle &= -\frac{4A}{\pi a^3}, \\
\langle --|V(r)|--\rangle &= -\frac{4A}{\pi a^3}.
\end{aligned} \tag{3.44}$$

squaring these and averaging we obtain

$$\frac{\delta}{2} = \frac{4\sqrt{3}A}{\pi a^3}. \tag{3.45}$$

Giving a probability of

$$P(\bar{M}) = 4.5 \times 10^3 \text{ GeV}^4 \times \left(\frac{g_{3l}}{M_\chi}\right)^4 \tag{3.46}$$

which agrees exactly with [11]. The authors of [11] then compare this to the probability given in [18] to find

$$\frac{M_\chi}{g_{3l}} > 290 \text{ GeV} \tag{3.47}$$

which we also find. However, the updated bounds as found by [27] give

$$\frac{M_\chi}{g_{3l}} > 2.6 \text{ TeV} \tag{3.48}$$

which again agrees with our findings.

Despite the overall agreement of our findings with those in the literature, there is some cause for concern. [11] find

$$\begin{aligned} \delta &= -\frac{8A}{\pi a^3} \quad \text{for the triplet state,} \\ \delta &= \frac{24A}{\pi a^3} \quad \text{for the singlet state} \end{aligned} \tag{3.49}$$

which is not what we find. The combined disagreement between the bilepton and model and the Feinberg-Weinberg model suggests that there is some element of this calculation that has not been properly accounted for. However, given the successful reproduction of the physically meaningful results from both models (namely, the correct Feinberg-Weinberg probability and bilepton mass bounds), it is clear that whatever the issue may be, it is a minor one, and the bounds for the N^0 can be trusted as we have obtained them.

3.A Appendix: Non-Relativistic Calculations

The goal of this appendix will be to explicitly illustrate how relativistic matrix elements $\mathcal{M}$ are expanded in the non-relativistic regime. Rather than attempt to explain it in complete generality, we will use the particular example of the N^0 matrix element $\mathcal{M}_s$. Before we begin, let us recall the relationship between the four-spinors $u(p), v(p)$ and the two-spinors ξ, η. In the Weyl basis, we have

$$u(p) = \begin{pmatrix} \sqrt{p \cdot \sigma}\ \xi \\ \sqrt{p \cdot \bar{\sigma}}\ \xi \end{pmatrix} \quad , \quad v(p) = \begin{pmatrix} \sqrt{p \cdot \sigma}\ \eta \\ -\sqrt{p \cdot \bar{\sigma}}\ \eta \end{pmatrix} \tag{3.50}$$

where σ^μ and $\bar{\sigma}^\mu$ are two-by-two matrices defined as

$$\sigma^\mu = (I, \boldsymbol{\sigma}) \quad , \quad \bar{\sigma}^\mu = (I, -\boldsymbol{\sigma}) \tag{3.51}$$

and $\{\sigma^i\}_{i=1}^3$ are the Pauli matrices. The first step will be to Taylor expand the momentum dependent coefficients of Equation 3.50 as

$$\begin{aligned} \sqrt{p \cdot \sigma} &\approx \sqrt{E}\left(1 - \frac{\mathbf{p} \cdot \boldsymbol{\sigma}}{2E} - \mathcal{O}[(\mathbf{p} \cdot \boldsymbol{\sigma})^2]\right) = \sqrt{m}\left(1 - \frac{1}{2}\mathbf{v} \cdot \boldsymbol{\sigma} + \mathcal{O}(v^2)\right) \\ \sqrt{p \cdot \bar{\sigma}} &\approx \sqrt{E}\left(1 + \frac{\mathbf{p} \cdot \boldsymbol{\sigma}}{2E} - \mathcal{O}[(\mathbf{p} \cdot \boldsymbol{\sigma})^2]\right) = \sqrt{m}\left(1 + \frac{1}{2}\mathbf{v} \cdot \boldsymbol{\sigma} + \mathcal{O}(v^2)\right) \end{aligned} \tag{3.52}$$

where m is the mass of the fermion in question and $\mathbf{v}$ is its velocity. Now, we will rotate to the Dirac basis using the unitary transformation

$$U = \frac{1}{\sqrt{2}} \begin{pmatrix} 1 & 1 \\ -1 & 1 \end{pmatrix} \tag{3.53}$$

such that

$$\gamma_{Dirac} = U \gamma_{Weyl} U^\dagger. \tag{3.54}$$

The advantage of this rotation is that in the Dirac basis, the dependence on velocity is not evenly distributed between the left and right handed portions of the four-spinor. Specifically, dropping all dependence of the spinors on velocity, they become in the Dirac basis,

$$u = \sqrt{2m} \begin{pmatrix} \xi \\ 0 \end{pmatrix} \quad , \quad v = -\sqrt{2m} \begin{pmatrix} 0 \\ \eta \end{pmatrix} \tag{3.55}$$

and

$$\bar{u} = \sqrt{2m}(\ \bar{\xi}\ ,\ 0\ )\quad ,\quad \bar{v} = \sqrt{2m}(\ 0\ ,\ \bar{\eta}\ ) \tag{3.56}$$

For this reason, it is in this basis that we will work. For reference, the γ-matrices expressed in the Dirac basis are

$$\gamma^0 = \begin{pmatrix} 0 & I \\ I & 0 \end{pmatrix}\quad ,\quad \gamma^k = \begin{pmatrix} 0 & \sigma^k \\ -\sigma^k & 0 \end{pmatrix}\quad ,\quad \gamma^5 = \begin{pmatrix} -I & 0 \\ 0 & I \end{pmatrix} \tag{3.57}$$

and the antisymmetric tensor is

$$\sigma^{\mu\nu} = \frac{i}{2}[\gamma^\mu, \gamma^\nu]\quad ,\quad \sigma^{0k} = \begin{pmatrix} 0 & i\sigma^k \\ i\sigma^k & 0 \end{pmatrix}\quad ,\quad \sigma^{ij} = \begin{pmatrix} \epsilon_{ijk}\sigma^k & 0 \\ 0 & \epsilon_{ijk}\sigma^k \end{pmatrix} \tag{3.58}$$

Now that we have all the necessary tools at our disposal, consider the matrix element corresponding to the s-channel contribution of the N^0 to muonium-antimuonium oscillation (Figure 3.1 and Equation 3.11)

$$\mathcal{M}_s = -\frac{g^2}{(\Lambda m_N)^2} k_\nu k_\beta g_{\mu\alpha} \bar{u}(p_4)\sigma^{\mu\nu} v(p_3)\bar{v}(p_1)\sigma^{\alpha\beta} u(p_2) \tag{3.59}$$

where we will neglect the mass of the electron in the expansion of

$$k_\mu = (p_1 + p_2)_\mu \approx (m_\mu, \mathbf{0}). \tag{3.60}$$

In order to tackle this carefully, let us start with the Lorentz vector

$$\begin{aligned} \bar{u}(p_4)\sigma^{\mu\nu} v(p_3) k_\nu &= m_\mu \bar{u}(p_4)\sigma^{\mu 0} v(p_3) \\ &= 2m_\mu \sqrt{m_e m_\mu}\ (\ \bar{\xi}_\mu\ ,\ 0\ ) \left[\begin{pmatrix} 0 & 0 \\ 0 & 0 \end{pmatrix}, \begin{pmatrix} 0 & i\sigma^k \\ i\sigma^k & 0 \end{pmatrix} \right] \begin{pmatrix} 0 \\ -\eta_e \end{pmatrix}, \end{aligned} \tag{3.61}$$

where in the last line we have written a Lorentz vector in square brackets, whose spatial component is a matrix in spin space, indicated with curly brackets. The four spinors then contract against this matrix such that each component of the Lorentz vector is a scalar in spin space. Continuing in such a fashion, we have

$$\begin{aligned}\bar{u}(p_4)\sigma^{\mu\nu}v(p_3)k_\nu &= 2m_\mu\sqrt{m_e m_\mu}[\ (0,0)\ ,\ (0,-i\bar{\xi}_\mu\sigma^k)\ ]\begin{pmatrix}0\\-\eta_e\end{pmatrix}\\ &= 2m_\mu\sqrt{m_e\mu}[0, i\bar{\xi}_\mu\sigma^k\eta_e].\end{aligned} \tag{3.62}$$

Similarly,

$$\begin{aligned}k_\beta\bar{v}_\mu(p_1)\sigma^{\mu\nu}u_e(p_2) &= m_\mu\bar{v}_\mu(p_1)\sigma^{\mu 0}u_e(p_2)\\ &= 2m_\mu\sqrt{m_e m_\mu}\,(\ 0\ ,\ \bar{\eta}_\mu\ )\left[0,\begin{pmatrix}0 & i\sigma^k\\ i\sigma^k & 0\end{pmatrix}\right]\begin{pmatrix}\xi_e\\0\end{pmatrix}\\ &= 2m_\mu\sqrt{m_e m_\mu}[0, -i\bar{\eta}_\mu\sigma^k\xi_e].\end{aligned} \tag{3.63}$$

Multiplying these terms, and remembering the minus sign that comes with $g_{\mu\nu}$, we get

$$\mathcal{M}_s = 4(m_\mu)^2(m_e m_\mu)\left(\frac{g}{\Lambda m_N}\right)^2\bar{\eta}_\mu\boldsymbol{\sigma}\xi_e\cdot\bar{\xi}_\mu\boldsymbol{\sigma}\eta_e. \tag{3.64}$$

We have almost reproduced the expression given in Section 3.1. However, it is important to note that when we make the comparison to the Born Approximation in Equation 3.5, we must also adjust our normalization conditions to be non-relativistic. This means dividing our expression by $4m_e m_\mu$ [22]. Finally, we obtain the correct expression:

$$\mathcal{M}_s = (m_\mu)^2\left(\frac{g}{\Lambda m_N}\right)^2\bar{\eta}_\mu\boldsymbol{\sigma}\xi_e\cdot\bar{\xi}_\mu\boldsymbol{\sigma}\eta_e. \tag{3.65}$$

3.B Appendix: The Probability of Muonium Decaying as Antimuonium

In this appendix we will go through the rigorous calculation of the probability for a muonium atom to decay as antimuonium. In the $\{|M\rangle, |\bar{M}\rangle\}$ basis, we have an interaction Hamiltonian, H_0, which

we can parametrize as

$$H_0 = \begin{pmatrix} E_M & \frac{\delta}{2} \\ \frac{\delta}{2} & E_{\bar{M}} \end{pmatrix}. \tag{3.66}$$

In such a situation, it is clear that the pure muonium and antimuonium states are not energy eigenstates. In fact, we have the eigenvector

$$|M_1\rangle = \frac{1}{[(w+\sqrt{w^2+\delta^2})^2+\delta^2]^{\frac{1}{2}}}[(w+\sqrt{w^2+\delta^2})|M\rangle + \delta|\bar{M}\rangle] \tag{3.67}$$

corresponding to the eigenvalue $\lambda_1 = \frac{1}{2}(E_M + E_{\bar{M}}) - \frac{1}{2}\sqrt{w^2+\delta^2}$ and a second eigenvector

$$|M_2\rangle = \frac{1}{[(w-\sqrt{w^2+\delta^2})^2+\delta^2]^{\frac{1}{2}}}[(w-\sqrt{w^2+\delta^2})|M\rangle + \delta|\bar{M}\rangle] \tag{3.68}$$

corresponding to the eigenvalue $\lambda_2 = \frac{1}{2}(E_M + E_{\bar{M}}) + \frac{1}{2}\sqrt{w^2+\delta^2}$ with $w = E_M - E_{\bar{M}}$. Suppose that at time $t = 0$ we have an atom in a pure muonium state. At some later time t, we can expect such an atom to now be in a state

$$\begin{aligned} |\psi(t)\rangle &= e^{-iHt}|M\rangle \\ &= e^{-iHt}(\langle M_1|M\rangle|M_1\rangle + \langle M_2|M\rangle|M_2\rangle) \\ &= a_1 e^{-i\lambda_1 t}|M_1\rangle + a_2 e^{-i\lambda_2 t}|M_2\rangle \end{aligned} \tag{3.69}$$

where

$$a_1 = \frac{w+\sqrt{w^2+\delta^2}}{[(w+\sqrt{w^2+\delta^2})^2+\delta^2]^{\frac{1}{2}}} \quad \text{and} \quad a_2 = \frac{w-\sqrt{w^2+\delta^2}}{[(w-\sqrt{w^2+\delta^2})^2+\delta^2]^{\frac{1}{2}}}. \tag{3.70}$$

We are most interested in the antimuonium component, which will be given by

$$\langle\bar{M}|\psi(t)\rangle = a_1 e^{-i\lambda_1 t}\langle\bar{M}|M_1\rangle + a_2 e^{-i\lambda_2 t}\langle\bar{M}|M_2\rangle. \tag{3.71}$$

The quantities $\langle\bar{M}|M_1\rangle$ and $\langle\bar{M}|M_2\rangle$ are quickly obtained from equations 3.67 and 3.68, giving

$$\langle \bar{M}|\psi(t)\rangle = \frac{\delta(w+\sqrt{w^2+\delta^2})}{(w+\sqrt{w^2+\delta^2})^2+\delta^2}e^{-i\lambda_1 t} + \frac{\delta(w-\sqrt{w^2+\delta^2})}{(w-\sqrt{w^2+\delta^2})^2+\delta^2}e^{-i\lambda_2 t} \tag{3.72}$$

which, after some algebra, can be reduced to

$$\begin{aligned}\langle \bar{M}|\psi(t)\rangle &= \frac{\delta}{2\sqrt{w^2+\delta^2}}[e^{-i\lambda_1 t} - e^{-i\lambda_2 t}] \\ &= -\frac{i\delta}{\sqrt{w^2+\delta^2}}e^{-\frac{i}{2}(E_M+E_{\bar{M}})t}\sin\left(\frac{t}{2}\sqrt{w^2+\delta^2}\right)\end{aligned} \tag{3.73}$$

The total probability for the atom to decay from its antimuonium state is given by the integral

$$\begin{aligned}P(\bar{M}) &= \int_0^\infty \Gamma e^{-\Gamma t}|\langle \bar{M}|\psi(t)\rangle|^2\, dt \\ &= \frac{\Gamma\delta^2}{w^2+\delta^2}\int_0^\infty e^{-\Gamma t}\sin^2[\frac{t}{2}\sqrt{w^2+\delta^2}]\, dt\end{aligned} \tag{3.74}$$

Where Γ is the muon decay constant. This integral can be done analytically and the result is, as agrees with [9],

$$P(\bar{M}) = \frac{\delta^2}{2(\Gamma^2+w^2+\delta^2)} \tag{3.75}$$

which we can approximate, given that $\Gamma >> (w^2+\delta^2)$, as

$$P(\bar{M}) \approx \frac{\delta^2}{2\Gamma^2} \tag{3.76}$$

Chapter 4

Model Building

4.1 Emergence of the Flavour-Mixing Signature

A very important aspect of the dipole operator is that it connects particles with left-handed helicity to particles with right-handed helicity (see Equation 1.16), and the reason this is important is that the electroweak sector of the SM is written in terms of an $SU_L(2)$ gauge symmetry, which is not respected by such an operator. At energies below the scale of electroweak symmetry breaking this is not an issue since this symmetry gets broken by the Higgs mechanism, but it means that there must be some higher energy theory which does respect $SU_L(2)$ invariance, from which our signature emerges as a low energy effective theory. A reasonable question to ask then is: what kind of theory could such a signature emerge from? We will provide one suggestion for a mechanism which enables this, though it should be noted that it is not necessarily a unique choice. Before we move forward, a few remarks on notation are in order. First, in this chapter, unlike in previous chapters, we will write fermionic fields as two-component Weyl fields instead of four-component Dirac fields. This is because the Standard Model is most succinctly expressed in terms of Weyl fields, rather than Dirac fields, due to the way that left-handed and right-handed fields are treated by the gauge bosons (for a brief overview of this structure, see Appendix A). We will make use of three matrices in this basis, that we shall define:

$$\begin{aligned} \sigma^{\mu} &= (I, \boldsymbol{\sigma}) \\ \bar{\sigma}^{\mu} &= (I, -\boldsymbol{\sigma}) \\ \sigma^{\mu\nu} &= \frac{i}{4}[\sigma^{\mu}, \sigma^{\nu}] \end{aligned} \tag{4.1}$$

where $\boldsymbol{\sigma}$ is defined in Equation 1.4. It is worth repeating that these are two-by-two matrices in spin-space and they will be acting on two-component spinors, in contrast to the Dirac matrices,

which are four-by-four. The signature of the N^0 considered here can then be written in terms of these Weyl fermions as

$$\mathcal{L}_{int} = \frac{g\eta}{2\Lambda}\bar{e}\sigma^{\mu\nu}\mu^c N_{\mu\nu} + \frac{g\eta}{2\Lambda}\bar{e^c}\sigma^{\mu\nu}\mu N_{\mu\nu} + H.C. \tag{4.2}$$

where e is the left-handed electron field, and μ^c is the right-handed muon field. To return to the question of what $SU_L(2)$ invariant theory might produce the N^0 signature as we have considered it, we consider an $SU_L(2) \times U_Y(1)$ invariant addition to the SM Lagrangian density of the form

$$\begin{aligned}\mathcal{L}_{eff} = \mathcal{L}_{kin} - M\bar{E}E^c + m_i\bar{E}e_i^c + \lambda_i(\bar{L}_i H)E^c \\ + \frac{1}{\Lambda}\bar{E}^c\sigma^{\mu\nu}EN_{\mu\nu} + y_{ij}(\bar{L}_i H)e_j^c + H.C.\end{aligned} \tag{4.3}$$

Where

- E and E^C are the left and right handed fields of a heavy vector-like fermion of mass M, which are singlets under $SU_L(2)$ and carry hypercharge $Y = -1$.
- $\mathcal{L}_{kin}$ contains the kinetic terms for the fermion fields E and E^C, and is given by

$$\mathcal{L}_{kin} = i\bar{E}\bar{\sigma}^\mu\partial_\mu E + i\bar{E}^c\sigma^\mu\partial_\mu E^c \tag{4.4}$$

- m_i, λ_i, and y_{ij} are mass terms with $\{i, j\}$ being indices over the fermion generations, $\{i, j\} = \{e, \mu, \tau\}$ for the electron, muon, and tauon generations, respectively.
- L_i and H are the $SU_L(2)$ doublets $\begin{pmatrix} \nu_i \\ e_i \end{pmatrix}$ and $\begin{pmatrix} \phi^+ \\ \phi^0 \end{pmatrix}$
- e_i^c are the right handed fermion singlets.
- Finally, the term $\frac{1}{\Lambda}(E^c)^\dagger\sigma^{\mu\nu}EN_{\mu\nu} + H.C.$ is included to embody higher order interactions between the vector-like fermion E and the N^0 boson, in exact analogy with equation 1.15.

The reader should be reminded that in our notation we are employing the Einstein summation convention, where repeated indices are summed over. So, for example, the expression

$$y_{ij}(\bar{L}_i H)e_j^c \tag{4.5}$$

really means

$$\sum_{i=1}^{3}\sum_{j=1}^{3} y_{ij}(\bar{L}_i H)e_j^c. \tag{4.6}$$

If we vary the Lagrangian in Equation 4.3 with respect to $\bar{E}$, we obtain the classical equations of motion,

$$i\sigma^\mu \partial_\mu E - ME^c + m_i e_i^c + \frac{1}{\Lambda}\sigma^{\mu\nu}E^c N_{\mu\nu} = 0. \tag{4.7}$$

We will now integrate out the heavy field E by considering energies much lower than the mass M. In such an energy regime, the momentum of the field E must be extremely small compared with M, so we will treat the ratio

$$\frac{i}{M}\sigma^\mu \partial_\mu E \approx 0. \tag{4.8}$$

This leaves us with

$$\left(1 - \frac{1}{M\Lambda}\sigma^{\mu\nu}N_{\mu\nu}\right) E^c = \frac{m_i}{M} e_i^c. \tag{4.9}$$

To solve this equation, we need the inverse of the matrix on the left hand side of E^c, and in general this is not a trivial task. However, since we are only interested in keeping terms which are first order in $(M\Lambda)^{-1}$, we can solve this with the matrix

$$\left(1 + \frac{1}{M\Lambda}\sigma^{\mu\nu}N_{\mu\nu}\right) \tag{4.10}$$

which yields

$$E^c = \frac{m_i}{M}\left(1 + \frac{1}{M\Lambda}\sigma^{\mu\nu}N_{\mu\nu}\right) e_i^c. \tag{4.11}$$

We can also vary Equation 4.3 with respect to $\bar{E}^c$, and solve for E in an identical way to find

$$E = \frac{\lambda_i}{M}\left(1 + \frac{1}{M\Lambda}\sigma^{\mu\nu}N_{\mu\nu}\right)(H^c)^\dagger L_i. \tag{4.12}$$

We can now substitute these expressions back into our original Lagrangian density to obtain

$$\mathcal{L}_{eff} = \left(\frac{\lambda_i m_j}{M} + y_{ij}\right)(\bar{L}_i H)e_j^c + \frac{\lambda_i m_j}{M^2\Lambda}(\bar{L}_i H)\sigma^{\mu\nu}e_j^c N_{\mu\nu} + H.C. \tag{4.13}$$

At this point, we recognize that when the Higgs field assumes its vacuum expectation value (VEV), what we will have is a mass term (the former) which is not diagonal in the generations, and a term very similar to our interaction of interest (the latter), but which is also not diagonal. The mass basis for the charged leptonic fields expresses physical states that we are working with, because these leptons do not spontaneously change generations. So, we will diagonalize the mass matrix, and uncover the form our interaction must take. Following [5], since the mass matrix

$$\kappa_{ij} = \left(\frac{\lambda_i m_j}{M} + y_{ij}\right) \tag{4.14}$$

is Hermitian, it can be diagonalized using unitary matrices, U (we will use indices $\{a, b, c\}$ to indicate the basis in which κ is diagonal):

$$\kappa_{ab} = U^L_{ia}\kappa_{ij}(U^R_{jb})^\dagger. \tag{4.15}$$

With this transformation in mind, we redefine the fields

$$\begin{aligned} H^\dagger L_i &\rightarrow (U^L_{ia})^\dagger H^\dagger L_a \\ e_i &\rightarrow (U^R_{ia})^\dagger e_a \end{aligned} \tag{4.16}$$

where U^R and U^L act on right-handed and left-handed fields. Substituting these into our Lagrangian density gives

$$\begin{aligned} \mathcal{L}_{eff} &= (\bar{L}_a H)U^L_{ia}\kappa_{ij}(U^R_{jb})^\dagger e_b^c + U^L_{ia}\frac{\lambda_i m_j}{M^2\Lambda}(U^R_{jb})^\dagger(\bar{L}_a H)\sigma^{\mu\nu}e_b^c N_{\mu\nu} + H.C. \\ &= \kappa_{ab}(\bar{L}_a H)e_b^c + U^L_{ia}\frac{\lambda_i m_j}{M^2\Lambda}(U^R_{jb})^\dagger(\bar{L}_a H)\sigma^{\mu\nu}e_b^c N_{\mu\nu} + H.C. \end{aligned} \tag{4.17}$$

Now, at energies below the electroweak symmetry breaking scale, the Higgs field takes on its VEV,

$$H = \begin{pmatrix} 0 \\ \\ \frac{1}{\sqrt{2}}v \end{pmatrix} \tag{4.18}$$

and leaves us with

$$\mathcal{L}_{eff} = \frac{v}{\sqrt{2}}\kappa_{ab}\bar{e}_a e_b^c + \frac{1}{\Lambda_{ab}}\bar{e}_a\sigma^{\mu\nu}e_b^c N_{\mu\nu} \tag{4.19}$$

$$\mathcal{L}_{int} = \frac{1}{\Lambda_{ab}}\bar{e}_a\sigma^{\mu\nu}e_b^c N_{\mu\nu} \tag{4.20}$$

where we have defined

$$\frac{1}{\Lambda_{ab}} = U_{ia}^L \frac{v\lambda_i m_j}{\sqrt{2}M^2\Lambda}(U_{jb}^R)^\dagger \tag{4.21}$$

to recognize that even though κ is diagonalized in this basis, the matrix in front of the interaction term is not, and so continues to mix the generations. In fact, the mixing terms of this interaction, $\{a = 1, b = 2\}$, are exactly the signature that we have been considering.

4.2 Generalized Leptonic Dipole Interaction

In addition to the leptonic signature of interest, this model also contains flavour diagonal terms which connect electrons to electrons and muons to muons (Λ_{11}, and Λ_{22} respectively).The implication is that Equation 4.3 has farther reaching consequences than the signature we have considered for the majority of this work. For example, it will contribute to the decay of the muon to three electrons; one of the rare decay paths mentioned in Section 1.1. We will take this opportunity to examine these contributions for the different mass scenarios of the N^0.

4.2.1 A Heavy N^0

If the N^0 boson is substantially heavier than the muon, then it will not be produced on shell in any muon decay event. However, the appearance of the generation-respecting terms in Equation 4.17 will mean that a heavy N^0 will create a path for the decay $\mu \to 3e$ as in shown in Figure 4.1. As

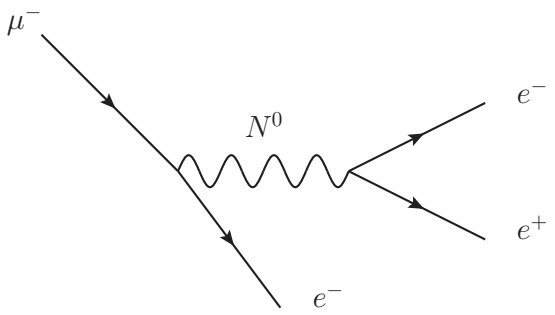

Figure 4.1: The decay of the muon into two electrons and a positron, facilitated by the generation preserving interaction of the generalized N^0 .

was mentioned, this decay path has never been observed and so there is a stringent bound on its branching ratio. We must gauge the size of this process given the constraints put on Λm_N in Section 2.2. The matrix element corresponding for Figure 4.1 scales as

$$\begin{aligned} |\mathcal{M}| &\sim \frac{1}{\Lambda_{11}\Lambda_{12}m_N^2} \\ &\approx \frac{1}{\Lambda^2 m_N^2} \end{aligned} \tag{4.22}$$

Where in the second line we recognize that even though Λ_{11} and Λ_{12} are distinct parameters, they will certainly be of the same magnitude, and so for the purposes of this calculation, maybe each be treated as approximately equal to the Λ of Equation 1.1. At this point, we will treat contributions from the electron mass as negligible. The general tree level expression for the decay rate is given by [5] as

$$\Gamma_\mu = \frac{1}{192\pi^3}|\mathcal{M}|^2. \tag{4.23}$$

By dimensional analysis, it is clear that the rate corresponding to the N^0 decay path scales as

$$\Gamma_{N^0} \sim \frac{1}{192\pi^3}\left(\frac{m_\mu^9}{\Lambda^4 m_N^4}\right) \tag{4.24}$$

The least stringent bound on the product Λm_N is given in Table 2.3 as $\Lambda m_N = 0.3$ TeV^2, which gives

$$\Gamma_{N^0} \approx 2 \times 10^{-35} \text{ GeV} \tag{4.25}$$

if we use the value for the the total muonic decay width from [19] of $\Gamma_{tot} \approx 3.0 \times 10^{-19}$ GeV, we obtain a branching ratio of

$$\frac{\Gamma_{N^0}}{\Gamma_{tot}} \approx 7 \times 10^{-17} \tag{4.26}$$

which is far below the current experimental constraint of $B(\mu \to 3e) = 10^{-12}$ (See Table 1.1). This is encouraging, as it means that even with the flavour respecting dipole transitions and their implications, a heavy N^0 may be a viable candidate for physics beyond the SM.

4.2.2 A Light N^0

The case of a light mediator is slightly more complicated and warrants two separate subcases. let us first consider the case where the N^0 is heavier than the muon, but still sufficiently light that the Equation 2.30 applies. In this case, the tree level decay path is the same as in the heavy case, but the matrix element now scales as

$$|\mathcal{M}| \sim \frac{1}{\Lambda^2}. \tag{4.27}$$

Using the same rationale as in the heavy case, we obtain a decay width of

$$\Gamma_{N^0} \sim \frac{1}{192\pi^3} \left(\frac{m_\mu^5}{\Lambda^4} \right). \tag{4.28}$$

The least stringent bound placed on Λ in Section 2.3 is $\Lambda = 4.0$ TeV, which gives a value for the decay width of

$$\Gamma_{N^0} \approx 7 \times 10^{-24}. \tag{4.29}$$

Comparing this with the total decay width gives a branching ratio of

$$\frac{\Gamma_{N^0}}{\Gamma_{tot}} \approx 2 \times 10^{-5} \tag{4.30}$$

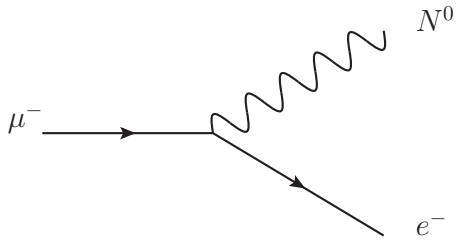

Figure 4.2: The decay of the muon into and electron and an on-shell N^0, facilitated by the flavour diagonal interactions present in equation 4.19. This decay route is possible only if the mass of the N^0 is lighter than that of the muon.

which is many orders of magnitude larger than the experimental constraint. Even with a largest bound of $\Lambda = 13$ TeV, we are still left with a branching ratio of

$$\frac{\Gamma_{N^0}}{\Gamma_{tot}} \approx 1 \times 10^{-7} \tag{4.31}$$

which is still much too large. In fact, in order for the light N^0 to match this probability, we must have $\Lambda \approx 275$ TeV, an energy scale which would require a a dedicated experimental search in order to properly probe.

We will make note of a third situation: the N^0 could have a mass which is less than the mass of the muon. In this case, the decay path is very different. Now, the N^0 can be produced on shell, and so the decay process actually looks like Figure 4.2. Though we will perform no calculations on this scenario, it may prove to be an interesting project in future work since any experiment looking for traces of such a decay would be met with some difficulty. Since the observed products are the same as the typical muon decay $\mu \to e^- \nu_\mu \bar{\nu}_e$, the only clear indication that something different is happening would be the energy of the emitted electron.

Another interesting aspect of the flavour diagonal interactions is that the N^0 now contribites to the scattering of $e^+e^- \to \mu^+\mu^-$ through an s-channel path. However, the chiral structure of the dipole interaction will not allow for interference with the SM processes, which means that such a contribution will be highly suppressed compared with the t-channel process looked at in Chapter 2. Any bounds obtained from this process will therefore be much smaller, and we omit this calculation.

Chapter 5

Conclusion and Discussion

5.1 Summary of Results

In this work we have considered the addition of a single neutral massive vector field N_μ to the Standard Model, which interacts with the electron and muon fields through a lepton flavour violating dipole term of the form

$$\mathcal{L}_{eff} = \frac{g\eta}{2\Lambda}\bar{e}\sigma^{\mu\nu}\mu N_{\mu\nu} + H.C., \tag{5.1}$$

where we adopt the convention of $g^2 = 4\pi$, $\eta = \pm 1$, Λ is the mass scale associated with the coupling, and we label the mass of the N^0 boson as m_N. We have analyzed the contribution of such a particle to the scattering process $e^+e^- \to \mu^+\mu^-$, to muonium-antimuonium oscillations, and to rare muon decays and obtained bounds on the relevant parameters.

In Chapter 2, we have considered two different scenarios for the contribution of such an interaction to e^+e^- scattering; one in which the mass of the N^0 is very large, and one in which the mass is very small, and obtained a variety of bounds for each of these cases by comparing to measurements of the cross section and forward-backward asymmetry from the LEP experiments. In the heavy case, it is only possible to set bounds on the product Λm_N, and the most stringent bound obtained comes from the cross section data, with $\eta = +1$, and gives the $\Lambda m_N > 2.0$ TeV^2. In the light case, a bound similar in magnitude to those on the four-fermion interactions comes from the cross section data, and gives $\Lambda > 13.0$ TeV. The methods used to obtain these bounds were then tested by reproducing the bounds set by LEP on a variety of four-fermion models [16]. Successful reproduction of their results validates the methodology used in obtaining limits for the various N^0 scenarios.

The muonium-antimuonium oscillations are analyzed in Chapter 3, and we have considered only the heavy scenario. We find that the bounds placed on the parameters from this process are much

less stringent than those placed on them by the scattering processes. Specifically, we find that the product $\Lambda m_N > 0.03$ GeV^2 in order that the probability of muonium decaying as antimuonium be kept below $P(\bar{M}) = 8.2 \times 10^{-11}$ as set by [27].

In Chapter 4, we recognize that the interaction governed by Equation 5.1 is not invariant under the $SU_L(2)$ gauge symmetry of the SM, and we propose one possible addition to the SM Lagrangian from which the flavour mixing signature emerges as a low energy effective theory. We find an interesting consequence of our model is the simultaneous existence of flavour diagonal transitions of the same form. Such a model would then also contribute to processes such as $e^+e^- \to e^+e^-$ scattering, among other things, and also contributes to the rare muon decay $\mu \to e^+e^-e^-$. We investigate the size of the contribution to this decay route for both the heavy and light case, and for bounds obtained from the scattering analysis find the heavy N^0 far below the experimental constraint on the branching ratio of $B(\mu \to 3e) = 10^{-12}$. This branching ratio for the light N^0 provides its most rigid constraint, with $\Lambda > 275$ TeV, and while this energy scale is not necessarily experimentally inaccessible in the near future, at present (and to the authors knowledge) there are no ongoing experiments designed to increase the bounds on the $\mu \to e^+e^-e^-$ branching ratio.

5.2 Future Prospects

We have neglected the calculation of the light N^0 to muonium-antimuonium oscillation, and it seems that this may be a more interesting calculation, possibly providing more stringent bounds than the ones obtained for the heavy N^0. It is also possible that the branching ratio for the rare muon decay from the light N^0 makes a light mediator an unlikely scenario, but we stress that the Lagrangian postulated at the beginning of Chapter 4 is simply one possible model, and not necessarily unique. Perhaps the requirement that the $SU_L(2)$ invariant theory also be renormalizable will lead to a more promising model for a light N^0.

Another aspect of this work that may lead to interesting results is the incorporation of the third leptonic generation. It would be possible to extend the interaction term in Equation 4.19 to include tauons, and while this would substantially increase the number of parameters at work, it would also increase the number of processes available for analysis: for example, the exotic tau decays such as $\tau^- \to \mu^- + \gamma$ or $\tau^- \to l^-l^-l^+$, all of which are less tightly constrained than the rare muon decays [19].

Finally, though we have only considered a neutral mediator, it is in principle also possible to write down dipole transitions involving doubly-charged mediators, which we might label as N^{++} and N^{--}, which connect muons to positrons, and electrons to antimuons. The addition of such particles will also increase the size of the parameter space being considered, but again may provide the flexibility for a light N^0 to be a viable candidate for physics beyond the SM.

5.3 Conclusions

The signature we have presented and analyzed here is, at the present time, not motivated by any empirical fact or data set, and for this reason we recognize its speculative nature. It is well understood, however that the origin of generational lepton flavour conservation in the Standard Model is unclear, as such preservation does not exist in the quark sector. The question of lepton flavour violation becomes more and more interesting as experiments like MEG [1] probe the existence of exotic decays, and bounds on four-fermion (and other more elaborate) interactions become tighter. An interesting aspect of the signature presented here is that the bounds we have placed on its parameters are significantly lower in some cases than those on other LFV models, and we present these findings in the hopes of motivating future research into the structure of the charged leptonic sector.

Appendix A

Appendix: A (Very) Brief Introduction to the Standard Model

The Standard Model is the single best tested theory in the history of science, and contains a quantitative description of all of the observed particles to date, and their interactions. As may be expected, it is full of intricate details, the vast majority of which we will neglect here. For detailed explanations and more rigorous treatments of the SM and its properties, the reader is directed to [5, 12, 22, 26] and [4]. The goal of this appendix is to provide a brief overview of a few aspects of the SM which the reader may find useful in approaching different sections of this thesis. We will roughly follow Chapter 2 of [4], including only the aspects deemed relevant.

The SM is written down as a quantum field theory which is invariant under the gauge symmetry group $SU_C(3) \times SU_L(2) \times U_Y(1)$. Here the C stands for colour, as this is the group associated with the quark sector, L is the set of interactions concerning only particles with left-handed helicity, and Y is the symbol given to the quantity *weak hypercharge*, or simply, hypercharge. For each generator of each of these groups, we associate a particular vector field; eight gluon fields for $SU_C(3)$, which we label G^{α}_{μ}, $\alpha = \{1, 2...8\}$, three W fields for $SU_L(2)$ which we label W^{a}_{μ}, $a = 1..3$, and one field for $U_Y(1)$ which we label B_{μ}.

In addition to these gauge fields, we also have fermion fields, and the properties of these are determined by their transformation properties under the various gauge groups. It is worth reiterating that the SM is most succinctly written down in terms of two-component Weyl spinors, as opposed to the four-component Dirac spinors. With this in mind, let us start with the leptons. There are a total of nine lepton fields, six left-handed fields and three right-handed fields, which we will represent as follows: L_i is a pair of left-handed fermion fields given by

$$L_i = \begin{pmatrix} \nu_i \\ \\ l_i \end{pmatrix} \tag{A-1}$$

that transforms as a doublet under the $SU_L(2)$ gauge group and have hypercharge $Y = -\frac{1}{2}$. Here, ν_i is the neutrino, l_i is the charged lepton, and i is over the generations with $i = 1$ corresponding the electrons, $i = 2$ corresponding to muons, and $i = 3$ corresponding to tauons. There are also three right-handed lepton fields which we will represent as e_i^c. These transform as singlets under $SU_L(2)$ and have hypercharge $Y = -1$. Both L_i and e_i^c transform as singlets under $SU_C(3)$. It is important to note that the SM does not contain right-handed neutrinos, though they do appear in various extensions.

There are also 12 quark fields. The left-handed fields are written as Q_i, with

$$Q_1 = \begin{pmatrix} u \\ \\ d \end{pmatrix} \quad , \quad Q_2 = \begin{pmatrix} c \\ \\ s \end{pmatrix} \quad , \quad Q_3 = \begin{pmatrix} t \\ \\ b \end{pmatrix} . \tag{A-2}$$

and also transforms as doublets under $SU_L(2)$ and possess hypercharge $Y = \frac{1}{6}$. Here, $\{u, d, c, s, t, b\}$ correspond to the up, down, charm, strange, top, and bottom quarks, respectively, and each of these fields transforms as a triplet under $SU_C(3)$. For example,

$$u = \begin{pmatrix} u_r \\ \\ d_g \\ \\ u_b \end{pmatrix} \tag{A-3}$$

where here $\{r, g, b\}$ correspond to the possible colour charges red, green, and blue. There are also six right-handed quark fields, U_i with $Y = \frac{2}{3}$ and D_i with $Y = -\frac{1}{3}$, which are singlets under $SU_L(2)$, but also triplets under $SU_C(3)$. The $SU_L(2)$ doublets are written in the basis where the third generator $T^3 = \frac{1}{2}\sigma^3$ is diagonal (these generators will be introduced again in Equation A-5), and it turns out that the electric charge of a field can be derived from the component of T^3 and the hypercharge by the relation

$$Q = Y + T^3. \tag{A-4}$$

So, for example, e_i has $Y = -\frac{1}{2}$ and $T^3 = -\frac{1}{2}$ giving $Q = -1$, exactly as we would expect for an electron, muon, or tauon.

The interactions of quarks and gluons is extremely complicated, and as none of these processes are related to any aspect of the work considered here, this is the last we will speak of them. We will henceforth focus on the leptonic sector of the SM.

The meaning of a theory being invariant under a certain symmetry group is that the Lagrangian be unchanged by a transformation of its fields by elements of the group. Specifically, we want a Lagrangian which is invariant under the following transformations:

$$\begin{aligned} L_i &\to \exp(-\frac{i}{2}\theta(x) + iT^a w^a(x))L_i \\ e_i^c &\to \exp(-i\theta(x) + iT^a w^a(x))e_i^c \\ W_\mu^a &\to W_\mu^a + \partial_\mu w^a(x) - [T^a, T^b]w^b(x) \\ B_\mu &\to B_\mu + \partial_\mu \theta(x) \end{aligned} \tag{A-5}$$

where here we have labeled $\theta(x)$ and $w^a(x)$ are arbitrary functions of spacetime, and $T^a = \frac{1}{2}\sigma^a$ are the generators of $SU_L(2)$. The most general renormalizable Lagrangian we can write down which is invariant under these transformations is [1] (following the labeling convention in [4])

$$\mathcal{L}_{fg} = -\frac{1}{4}B_{\mu\nu}B^{\mu\nu} - \frac{1}{4}W^a_{\mu\nu}W^{a\ \mu\nu} - \frac{i}{2}\bar{L}_i\bar{\sigma}^\mu D_\mu L_i - \frac{i}{2}\bar{e}_i^c\sigma^\mu D_\mu e_i^c \tag{A-6}$$

where $\sigma^\mu, \bar{\sigma}_\mu$ are defined in Equation 4.1 and we have defined the gauge invariant field strength tensors

$$\begin{aligned} B_{\mu\nu} &= \partial_\mu B_\nu - \partial_\nu B_\mu \\ W^a_{\mu\nu} &= \partial_\mu W^a_\nu - \partial_\nu W^a_\mu + g_2[W^a_\mu, W^b_\mu]W^b_\nu, \end{aligned} \tag{A-7}$$

and the covariant derivatives

$$\begin{aligned} D_\mu L_i &= \left(\partial_\mu + \frac{i}{2}g_1 B_\mu - ig_2 T^a W^a_\mu\right) L_i \\ D_\mu e_i^c &= \left(\partial_\mu - ig_1 B_\mu - ig_2 T^a W^a_\mu\right) e_i^c, \end{aligned} \tag{A-8}$$

and the factors g_1, g_2 are the coupling strengths of the fermions to the $U_Y(1)$ and $SU_L(2)$ gauge

[1] Actually there are two more terms which are proportional to $\epsilon^{\mu\nu\alpha\beta}$, but these are very small and for the sake of compactness we shall ignore them.

fields respectively.

An important aspect of the SM as it is written is that no mass terms are permitted by the requirement of gauge invariance. In the charged lepton case, a term like $m_e \bar{L}_1 e_1^c$ would not be invariant under either $SU_L(2)$ (it is not a scalar in weak space) or $U_Y(1)$ (since this would transform into $\text{Exp}(-\frac{i}{2}\theta(x))\bar{L}_1 e_1^c$ under the fermionic transformations in Equation A-5). It is also clear that a mass term for the gauge bosons would clearly not be invariant under their transformations since nowhere would there be the necessary factors to cancel the terms quadratic in $\theta(x)$ or $w^a(x)$. The most obvious problem with such a theory, then, is that it is an experimental fact that charged fermions and three of the gauge bosons we know of have mass. What is the best way to reconcile this conflict? The solution to this problem was developed independently by several scientists, but is named after Peter Higgs, and is referred to generally as the *Higgs mechanism*. In the SM, the trick is to introduce a scalar field ϕ (called the Higgs field) defined as

$$H = \begin{pmatrix} \phi^+ \\ \\ \phi^0 \end{pmatrix} \tag{A-9}$$

which transforms as a doublet under $SU_L(2)$ and has hypercharge $Y = \frac{1}{2}$, and couple it to the fermions using Yukawa potentials. Specifically, for leptons, we add to the Lagrangian in Equation A-6

$$\mathcal{L}_{Higgs} = \mathcal{L}_H - f_{ij}(\bar{L}_i H)e_j^c + H.C. \tag{A-10}$$

where $\mathcal{L}_H$ is the kinetic and potential terms for the Higgs field, and f_{ij} are the Yukawa coupling constants. We then choose the potential in such a way that it is minimized at a non-zero value. This value, which we refer to as a *vacuum expectation value* or VEV, will spontaneously break the gauge symmetry. In the SM we perturb the Higgs about its VEV to get

$$H = \begin{pmatrix} 0 \\ \\ \frac{1}{\sqrt{2}}(v + \phi) \end{pmatrix} \tag{A-11}$$

where v is the Higgs VEV, and defines the scale at which the electroweak symmetry breaking occurs, and ϕ is the excitation known as the Higgs boson. We now have

$$\mathcal{L}_{Higgs} = \mathcal{L}_{\phi} - f_{ij}\frac{v}{\sqrt{2}}e_i e_j^c + H.C. \tag{A-12}$$

where $\mathcal{L}_{\phi}$ contains all of the terms involving the Higgs boson, and the remaining terms are the lepton mass matrix which, when diagonalized, will endow our charged leptons with mass.

To address the matter of how the gauge fields acquire mass, we must return to the energy scales above spontaneous symmetry breaking. Recall that in the electroweak sector, we have four gauge fields W_μ^a and B_μ, and a complex Higgs doublet, amounting to four real scalar fields. The Higgs field interacts with these gauge fields through its covariant derivative, given by

$$D_\mu H = (\partial_\mu - g_2 W_\mu^a T^a - \frac{i}{2}g_1 B_\mu)H \tag{A-13}$$

whose square is contained in $\mathcal{L}_{Higgs}$ to imbue the Higgs field with dynamics. At scales below electroweak symmetry breaking the Higgs takes on its VEV and causes the gauge fields to mix. This mixing leads to three of the four gauge fields becoming massive. Specifically, we end up with the new fields

$$W_\mu^{\pm} = \frac{1}{\sqrt{2}}\left(W_\mu^1 \mp iW_\mu^2\right) \tag{A-14}$$

obtaining a mass of

$$M_W = \frac{g_2 v}{2}. \tag{A-15}$$

It is conventional to parametrize the mixing of the remaining two fields B_μ and W_μ^3 with the *Weinberg angle* which is defined by the matrix

$$\begin{pmatrix} A_\mu \\ Z_\mu \end{pmatrix} = \begin{pmatrix} \cos\theta_W & \sin\theta_W \\ -\sin\theta_W & \cos\theta_W \end{pmatrix} \begin{pmatrix} B_\mu \\ W_\mu^3 \end{pmatrix}, \tag{A-16}$$

where the field A_μ remains massless after the symmetry breaking, and becomes the field associated with the U(1) gauge invariance of electromagnetism. Like the mass of the W bosons, the Weinberg angle can be expressed in terms of the fermionic couplings by the expressions

$$\begin{aligned} \cos\theta_W &= \frac{g_2}{\sqrt{g_1^2+g_2^2}}, \\ \sin\theta_W &= \frac{g_1}{\sqrt{g_1^2+g_2^2}}. \end{aligned} \tag{A-17}$$

From looking at the mass terms resulting form the symmetry breaking in [4], we can infer a further result,

$$\frac{M_W}{M_Z} = \cos\theta_W, \tag{A-18}$$

which means that because of the specific way that the Higgs field breaks the $SU_L(2)$ symmetry, the masses of the resulting bosons are not independent. For further details on this, the reader is encouraged towards Chapter 2 of [4]. Because of this dependence, experimental bounds are set on combinations of the masses. In particular, [19] gives

$$m_Z - m_W = 10.4 \pm 1.6 \text{ GeV} \tag{A-19}$$

as the current most precise experimental value.

Bibliography

[1] J. Adam et al. New limit on the lepton-flavour violating decay $\mu^+ \to e^+\gamma$. *Phys.Rev.Lett.*, 107:171801, 2011.

[2] A.B. Arbuzov, M. Awramik, M. Czakon, A. Freitas, M.W. Grunewald, et al. ZFITTER: A Semi-analytical program for fermion pair production in e+ e- annihilation, from version 6.21 to version 6.42. *Comput.Phys.Commun.*, 174:728–758, 2006.

[3] G. Bohm and Gunter Zech. Introduction to statistics and measurement analysis for physicists. 2005.

[4] C.P. Burgess and G.D. Moore. The standard model: A primer. 2007.

[5] W.N. Cottingham and D.A. Greenwood. An introduction to the standard model of particle physics. 2007.

[6] S.P. Das, F.F. Deppisch, O. Kittel, and J.W.F. Valle. Heavy Neutrinos and Lepton Flavour Violation in Left-Right Symmetric Models at the LHC. *Phys.Rev.*, D86:055006, 2012.

[7] Malcolm J. Duncan, J.A. Grifols, A. Mendez, and S. Uma Sankar. RESTRICTIONS ON THE NEUTRINO MAGNETIC DIPOLE MOMENT. *Phys.Lett.*, B191:304, 1987.

[8] E. Eichten, Kenneth D. Lane, and Michael E. Peskin. New Tests for Quark and Lepton Substructure. *Phys.Rev.Lett.*, 50:811–814, 1983.

[9] G. Feinberg and S. Weinberg. Conversion of Muonium into Antimuonium. *Phys.Rev.*, 123:1439–1443, 1961.

[10] Paul H. Frampton. Bileptons: Status and prospects. *Int.J.Mod.Phys.*, A13:2345–2350, 1998.

[11] H. Fujii, S. Nakamua, and K. Sasaki. Constraints on dilepton mass from low-energy muon experiments. *Phys.Lett.*, B299:342–344, 1993.

[12] David Griffiths. Introduction to elementary particles. 2008.

[13] Peter Herczeg and Rabindra N. Mohapatra. Muonium to anti-muonium conversion and the decay mu+ —gt; e+ anti-neutrino neutrino in left-right symmetric models. *Phys.Rev.Lett.*, 69:2475–2478, 1992.

[14] Chiu Man Ho and Robert J. Scherrer. Anapole Dark Matter. 2012.

[15] E.M. Lifshitz L.D. Landau. The classical theory of fields. 1951.

[16] C. Geweniger et al. LEPEWWG $f\bar{f}$ SubGroup.

[17] L. Lyons. STATISTICS FOR NUCLEAR AND PARTICLE PHYSICISTS. 1986.

[18] B.E. Matthias, H.E. Ahn, A. Badertscher, F. Chmely, M. Eckhause, et al. New search for the spontaneous conversion of muonium to anti-muonium. *Phys.Rev.Lett.*, 66:2716–2719, 1991.

[19] K. Nakamura et al. Review of particle physics. *J.Phys.G*, G37:075021, 2010.

[20] Yasuhiro Okada. Searching for new physics through LFV processes. *J.Korean Phys.Soc.*, 45:S467–S471, 2004.

[21] Sergio Pastor, Saurabh D. Rindani, and J.W.F. Valle. Lepton flavor violation in a left-right symmetric model. *JHEP*, 9905:012, 1999.

[22] Michael E. Peskin and Daniel V. Schroeder. An Introduction to quantum field theory. 1995.

[23] Martti Raidal. Bileptons: Present constraints and future prospects at colliders. 1997.

[24] M.B. Tully and Girish C. Joshi. Mass bounds for flavor mixing bileptons. *Phys.Lett.*, B466:333, 1993.

[25] N.G. Unel. Lepton flavor violation at LHC. 2005.

[26] Steven Weinberg. The quantum theory of fields. Vol. 2: Modern applications. 1996.

[27] L. Willmann, P.V. Schmidt, H.P. Wirtz, R. Abela, V. Baranov, et al. New bounds from searching for muonium to anti-muonium conversion. *Phys.Rev.Lett.*, 82:49–52, 1999.